

DEVELOPMENT OF SPUTTERED TITANIUM NITRIDE LAYER FOR PASSIVATION OF SILICON SOLAR CELL.

A dissertation

submitted in partial fulfilment of the requirements for the degree of

**INTEGRATED MASTER OF TECHNOLOGY
IN
ENERGY ENGINEERING**

By

AISHIK BASU MALLICK

CUJ/I/2014/IEE/014



**DEPARTMENT OF ENERGY ENGINEERING
CENTRAL UNIVERSITY OF JHARKHAND
BRAMBE, RANCHI**

MAY 2019



Central University of Jharkhand

(Established by Act of Parliament of India, 2009)

Department for Energy Engineering

Brambe, Ranchi, Jharkhand-835205

Certificate of Approval

The foregoing thesis by **Mr. Aishik Basu Mallick** Regn. No. **CUJ/I/2014/TEE/014** is hereby approved as a creditable study carried out and presented in a manner satisfactory to warrant its acceptance as a pre-requisite to the degree for which it has been submitted. It is understood that by this approval the undersigned do not necessarily endorse or approve any statement made, opinion expressed or conclusion drawn therein but approve only for the purpose for which it is submitted.

Committee On

Final Examination for

Evaluation of Thesis

CERTIFICATE

This is to certify that Aishik Basu Mallick, CUJ/I/2014/IEE/014, student of Integrated M.Tech in Energy Engineering, has worked on “**Development of Sputtered Titanium Nitride Layer for Passivation for Passivation of Silicon Solar Cell**”. This report is being submitted to Department of Energy Engineering, Central University of Jharkhand, Ranchi in partial fulfilment of requirement for the award of the degree of M.Tech in Energy Engineering, is an original contribution with existing knowledge and faithful record of work carried out by him under my guidance.

To the best of my knowledge this will be submitted as a part of his final M.Tech Project Dissertation and has not been submitted in part or full for any Degree Diploma to this University or elsewhere.

Central University of Jharkhand

Place: Ranchi

Dr.P. Prathap
(External Supervisor)
Scientist
CSIR-NPL, New Delhi

Dr. Bishnu Mohan Jha
(Internal Supervisor)
Assistant Professor
Central University of Jharkhand

Acknowledgement

I am thankful to my external supervisor **Dr. P.Prathap** for his expert guidance and allowing me to work on this topic. During the course of project his necessary tips and understanding of instruments helped me a lot to carry out experiments in a perfect manner.

I would like to express my sincere gratitude to honourable group head **Mr. C.M.S Rauthan** and other senior scientists **Dr. Sanjay kr.Srivastava , Dr Vandana** and other research colleagues at NPL for their valuable support throughout the course of 1 year.

I would be always indebted to **Dr.Mrinal Dutta** (Ramanujan Fellow,CSIR-NPL), for his unparallel support and motivation which helped me in the toughest of my time. He kept encouraging me to look forward towards unexplored areas.

I would always be grateful to **Dr. S.K Samdarshi**, Head of Centre for Engineering for the unending support he has provided, be it any need and at any time all throughout the 5 years of my course. I would like to make a special thanks to my colleges and Department, Dr. Bishnu Mohan Jha, Dr. Basudev Pradhan and P.S. Panja, all other faculty members for their recommendation and much needed motivation to work in CSIR-NPL

A research work is a combined effort of an efficient team to make it worth. I am thankful to all people at PV metrology group for their constant effort to support me mentally and also during my experiments. A special thanks to all research scholar Avritti di, Shweta Mam , Meenakshi Di, Pragya Mam, Veenu di Nitin for their help whenever it is needed the most.

I also thank Shrestha and Indranil for supporting me always and to be my side whenever is needed

I would also like to thank my parents for their support and encouragement to achieve desired goals.

.

Contents

| | |
|--|-----------|
| Abbreviations | <i>i</i> |
| List of Figures | <i>ii</i> |
| List of Tables | <i>iv</i> |
| Abstract | |
| Chapter 1: Introduction | |
| 1.1 The Need for Renewables | 1 |
| 1.2 Renewable Energy Global Scenario | 2 |
| 1.3 Solar Energy | 3 |
| 1.3.1 Harvesting Technology | 3 |
| 1.3.1.1 Solar Thermal Technology | 3 |
| 1.3.1.2 Photovoltaic Systems | 4 |
| 1.4 Solar Cells | 4 |
| 1.4.1 Short Circuit Current (I_{sc}) | 5 |
| 1.4.2 Open Circuit Voltage (V_{oc}) | 5 |
| 1.4.3 Fill Factor(FF) | 6 |
| 1.4.4 Efficiency | 6 |
| 1.5 Losses in Solar Cell | 7 |
| 1.5.1 Optical Losses | 7 |
| 1.5.2. Electrical Losses | 8 |
| 1.5.2.1 Ohmic Losses | 8 |
| 1.5.2.2 Recombination Losses | 8 |
| 1.6 Transition Metal Nitrides | 10 |
| 1.7 Metal Insulated Semiconductor(MIS) Structure | 11 |
| 1.7.1 C-V characteristics of MIS Device | 12 |
| 1.7.2 Defects | 14 |
| 1.7.3 Effect of C-V Direction in the C-V curve | 15 |
| 1.7.4 Conductance Method | 15 |
| 1.8 Aim of the present Work | 15 |

Chapter 2 : Thin Film Deposition Process and Characterization Techniques

| | |
|---|----|
| 2.1 Thin Film Deposition Process | 17 |
| 2.1.1 Introduction | 17 |
| 2.1.2 Thin Film Deposition Techniques | 18 |
| 2.1.2.1 Chemical Vapour Deposition (CVD) | 19 |
| 2.1.2.2 Physical Vapour Deposition (PVD) | 20 |
| 2.1.2.2.1 Evaporation | 20 |
| 2.1.2.2.1.1 Thermal Evaporation | 20 |
| 2.1.2.2.1.2 The Electron Beam Technique | 21 |
| 2.1.3 Sputtering | 22 |
| 2.1.3.1 Mechanism of Sputtering | 23 |
| 2.1.3.2 Advantage of Sputtering over other Methods | 24 |
| 2.1.3.3 Components of Sputtering | 26 |
| 2.1.3.4 Sputtering Parameters | 28 |
| 2.1.4 Preparation of Sample | 29 |
| 2.1.4.1 Cleaning | 29 |
| 2.1.4.2 Sputtering Process for TiN Thin Films | 30 |
| 2.1.4.3 Annealing of TiN deposited Silicon Samples | 31 |
| 2.1.4.4 Metallization | 31 |
| 2.2 Characterization Techniques | 32 |
| 2.2.1 UV-Vis-NIR Spectroscopy | 32 |
| 2.2.2 Electrostat/Potentiostat | 35 |
| 2.2.2.1 Electrochemical Impedance Spectroscopy | 36 |
| 2.2.3 Quantum Efficiency (QE) and Current Density (Jsc) | |
| Voltage (V) Measurement | 37 |

Chapter 3: Results and Discussion

| | |
|--|----|
| 3.1 Optical Measurement | 39 |
| 3.1.1 Transmission with Nitrogen Flow rate | 39 |
| 3.1.2 Transmission with Deposition Time variation | 39 |
| 3.2 C-V curves of the Samples | 40 |
| 3.2.1 Influence of Nitrogen flow rate | 40 |
| 3.2.1.2 Influence of Hydrogen annealing on flat-band voltage | 42 |

| | |
|--|----|
| 3.2.1.3 Nature of Traps | 43 |
| 3.2.1.4 Effect of Traps at the interface | 46 |
| 3.2.2 Influence of thickness on Si/TiN interface | 48 |
| 3.2.2.1 Influence of annealing | 50 |
| 3.2.2.2 Nature of Traps | 51 |
| 3.2.2.3 Effect of Traps at the interface | 52 |
| 3.2.3 Leakage Current Characteristics | 54 |

Chapter 4: Passivation effect of sputtered deposited TiN layer

| | |
|---|----|
| 4.1 Introduction | 55 |
| 4.2 Experimental | 55 |
| 4.2.1 Preparation of Silicon Solar Cell | 55 |
| 4.2.2 Device Characterization | 56 |
| 4.3 Results and Discussion | 56 |

| | |
|------------------------------------|-----------|
| Conclusions and Future Work | 58 |
|------------------------------------|-----------|

| | |
|------------|--|
| References | |
|------------|--|

Abbreviation

| | |
|------------------|--|
| SRH | Shockley –Read- Hall |
| PV | Photovoltaic |
| Dit | Interface Defect Density |
| Q _{eff} | Fixed Charge Density |
| V _{fb} | Flat Band Voltage |
| MIS | Metal Insulated Semiconductor |
| UV | Ultraviolet Region |
| NIR | Near Infrared Region |
| EIS | Electrochemical Impedance Spectroscopy |
| QE | Quantum Efficiency |
| J _{sc} | Short Circuit Current |
| V _{oc} | Open Circuit Voltage |
| FF | Fill Factor |
| AM | Air Mass |
| SCCM | Standard Cubic Centimetre per Minute |
| C-V | Capacitance Voltage |

List of Figures

| | | |
|----------|---|-------|
| Fig 1-1 | Comparison of present trends for Energy Generation for Different Sources | 2 |
| Fig 1-2 | Construction of a solar cell | 4 |
| Fig 1-3 | Curve showing I_{sc} , V_{oc} and P_{max} from the solar cell | 5 |
| Fig 1-4 | Different voltage and current points in I-V Curve | 6 |
| Fig 1-5 | Summary of losses occur in a solar cell | 7 |
| Fig 1-6 | Reflection Losses at the Surface | 8 |
| Fig 1-7 | Representation of two types of passivation scheme(a) chemical passivation (b) field effect passivation | 9 |
| Fig 1-8 | Metal Insulator Semiconductor in cross section view | 11 |
| Fig 1-9 | Capacitance of a MOS capacitor under various bias condition(a)Equivalent MOS device in terms of Capacitance. Capacitance as seen in (b) accumulation regime (c) Depletion regime (d) Inversion Low Frequency (e) Inversion High Frequency | 12 |
| Fig 1-10 | Normalized Capacitance Vs. Gate voltage for low frequency and high frequency | 13 |
| Fig 1-11 | Different types of Defects exist in MIS Device | 14 |
| Fig 2-1 | Thin and thick film regimes | 18 |
| Fig 2-2 | Schematic showing thermal evaporation | 21 |
| Fig 2-3 | Mechanism for e-beam evaporation | 22 |
| Fig 2-4 | Schematic of sputtering Process | 23 |
| Fig 2-5 | Mechanism of particle interaction at the target | 24 |
| Fig 2-6 | Schematic of mechanism of RF-Sputtering | 25 |
| Fig 2-7 | DC Magnetron Sputtering for TiN thin film deposition | 28 |
| Fig 2-8 | Shutter and Target in a Magnetron Gun Assembly | 29 |
| Fig 2-9 | Interference from thin film deposited on thick substrate, $s \gg d$ | 32 |
| Fig 2-10 | UV-Vis-NIR Spectrophotometer, (Make : Perkin Elmer Lambda 1050) | 33 |
| Fig 2-11 | Inside the spectrophotometer | 34 |
| Fig 2-12 | Electrostat/Potentiostat Gamry Instruments Reference 600 Model | 36 |
| Fig 2-13 | I-V and SR Measurement System, M/s Bunkoukeiki (Model: CEP-25HS 50) | 38 |
| Fig 3-1 | Transmission (%) for different nitrogen flow | 39 |
| Fig 3-2 | Transmission (%) for different deposition Time | 40 |
| Fig 3-3 | Combined C-V curve at 1 MHz of (a) as deposited and (b) annealed with flow rate | 40 |
| Fig 3-4 | (a) Effective charge Density Vs. Flow rate of r as deposited and annealed (b) Flat Band Voltage Vs. Nitrogen Flow for as deposited and annealed | 41 |
| Fig 3-5 | Dit values for various nitrogen flow | 41 |
| Fig 3-6 | C-V curve comparison between as deposited with annealed at 1Mhz | 43 |
| Fig 3-7 | Trends in C-V curve of as deposited for different frequency with flow rate variation | 44 |
| Fig 3-8 | C-V curve with different frequency variation for annealed samples with flow rate | 45 |
| Fig 3-9 | Effect of sweep direction for as deposited samples with flow rate | 46-47 |
| Fig 3-10 | Effect of sweep direction for annealed samples with flow rate | 47-48 |
| Fig 3-11 | Comparison of C-V as deposited and annealed with variation in time | 48 |
| Fig 3-12 | Trends in as deposited and annealed for (a) Effective Charge Density (B) Flat band shift with time | 49 |
| Fig 3-13 | Dit Values for different deposition time | 49 |
| Fig 3-14 | C-V for as deposited and annealed at 1MHz with deposition time variation | 50 |
| Fig 3-15 | C-V curve with different frequency variation for as deposited samples with deposition time | 51 |

| | | |
|----------|---|-------|
| Fig 3-16 | C-V curve with different frequency for annealed samples with deposition time | 52 |
| Fig 3-17 | Effect of Sweep direction for as deposited with change in deposition time | 52-53 |
| Fig 3-18 | Effect of Sweep direction for annealed with change in deposition time | 53 |
| Fig 3-19 | Leakage Current variation with (a) nitrogen flow rate and (b) deposition time for as deposited and annealed | 54 |
| Fig 4-1 | Current density Vs. voltage characteristics of solar cells (a) without passivation and with passivation (as deposited) (b) without passivation and with passivation (annealed) under AM1.5G solar | 56 |
| Fig 4-2 | EQE of solar cells (a) without passivation and with passivation (as deposited) (b) without passivation and with passivation (annealed) under AM1.5G solar illumination | 57 |

List of Tables

| | | |
|-----------|---|----|
| Table 1-1 | Global Renewable Energy Potential(Exajoules per Year) | 3 |
| Table 2-1 | Thin Film Property and its respective application | 17 |
| Table 2-2 | Parameters used for film deposition in DC Magnetron Sputtering | 30 |
| Table 3-1 | Qeff,Dit and Vfb values for as deposited and annealing samples for different flow rate | 41 |
| Table 3-2 | Qeff,Dit and Vfb values for as deposited and annealing samples for variation in deposition time | 49 |
| Table 3-3 | Values for Leakage Current for different Nitrogen Flow | 54 |
| Table 3-4 | Values for Leakage Current for different deposition time | 54 |
| Table 4-1 | Solar Cell Parameters of passivated and unpassivated solar cells | 57 |

Abstract

In order to achieve high efficiency of solar cells, surface recombination losses should be minimized. This surface loss becomes vital in case of present nanostructured solar cell. There are different types of material that can be used as passivation layer such as SiN_x , SiO_2 , Al_2O_3 etc. These type of material are much common and are extensively explored. Compared to these previously explored materials TiN is much more new and still not explored as a passivation layer. TiN also comes with some other interesting properties such as corrosion resistant layers, biocompatible and diffusion barriers for electronic devices etc. Also there are different techniques which so far used to deposit passivation layer such as Atomic Layer Deposition Process, Plasma Enhanced Chemical Vapour Deposition (PECVD), Sputtering etc. Sputtering is a developed technology for thin film preparation at relatively lower cost and operationally simple.

In this dissertation work, deposition of TiN layer by sputtering process has been carried out and characterization is done to optimize its properties and successful implementation of TiN as a passivation layer on solar cells is also carried out. The overall work is divided into four chapters which are as follows.

Chapter-1 : This chapter contains information about the basic parameters of solar cell, different loss mechanism in solar cells, different properties of TiN layers and some details about the device structure (MIS) used to find defect density of TiN layer.

Chapter-2 : This chapter presents the different deposition techniques used to deposit thin films and also the different characterization techniques used in the dissertation work to characterize the samples.

Chapter – 3 : This chapter contains information about the capacitance voltage measurement of the samples. This measurement includes information about the defect density, fixed charge density, effect of frequency variation on C-V curves etc.

Chapter – 4: This Chapter presents the solar cell fabrication technique and the deposition of TiN layer over the solar cells. The passivation effect has been analysed by measuring the current density versus voltage characteristics and EQE of the solar cells,

CHAPTER-1

Introduction

1.1 The Need for Renewables.

The living standards of the 21st century has been revolutionized by the technological advancements in the last 30 years. Starting from dawn to dusk, we all are surrounded by tons of gadgets , equipment's in order to complete the daily task. Everything around us need energy to perform the specified task for which it is created. Energy is vital resource for wide range of applications such as household requirements, industrial, transportations and agricultural applications The primary sources of energy are petroleum natural gas coal and wood except the wood all other have the finite supply. These fossil fuels being non sustainable will eventually deplete and have ill side effects on their users. When these fossil fuels are burnt it produces a large amount of harmful gases mostly carbon dioxide, methane, nitrous oxide, hydrocarbons are emitted in the atmosphere. This is the main cause of global warming that in turn increases the temperature of the planet and endangering the life of species that resides on the earth. Beside the temperature rise this deleterious gases give birth to air pollution causing reduced growth of human health and plant, acid rain that destroys marble monument as seen in Taj Mahal. Extraction of coal by mining leaves the land barren and also makes the soil infertile for further use. The disastrous effect of Deep Water Horizon oil rig under the ocean floor incident is a live example of extraction of oil for energy use. Its also effected the marine ecosystem largely. Also the oil crisis of 1973 is the first event that embarks the possibility of energy crisis in the near future. This event in 1970's led to the motivation for the world to look for alternate source of energy.

With the exponential increase in the population growth, the thrust and the need for energy is also rapidly increasing and these increase is causing a havoc demand on the fossil fuels to meet requirement. These fossil fuel are depleting at a faster rate so a positive attitude should be tried at every level to replace fossil fuels with renewable energy as the main source of generating energy.

Renewable energy is the energy that is derived from a limitless source. With Proper infrastructure this source of energy is clean stable cost effective efficient and has reduced environmental effects The major source of the renewable energy are solar energy wind geothermal biomass hydro power tidal energy etc. These energy sources has almost negligible amount of carbon emission and will help to cure in some extent the climate change that is caused by fossil fuel burning.

Therefore as these non-renewable are consumed, human beings also pay particular tension for some long term permanent sources of energy. The economic instability of the oil prices also creates rising concern towards the use of conventional sources in the future. So a thrust is needed towards these renewables to reduce dependency on conventional and thus saving the nature.

1.2 Renewable Energy Global Scenario

Renewables energy are not new, it is well utilized from ancient times for producing energy but at a smaller scale. In 1970 the oil crisis due to various political problems highlighted the need of the renewable energy particularly the solar energy. The present scenario also speaks the same story. It is seen that the theoretical as well as practical potential of solar energy is high as compared to other renewable energy sources.(Table1-1)

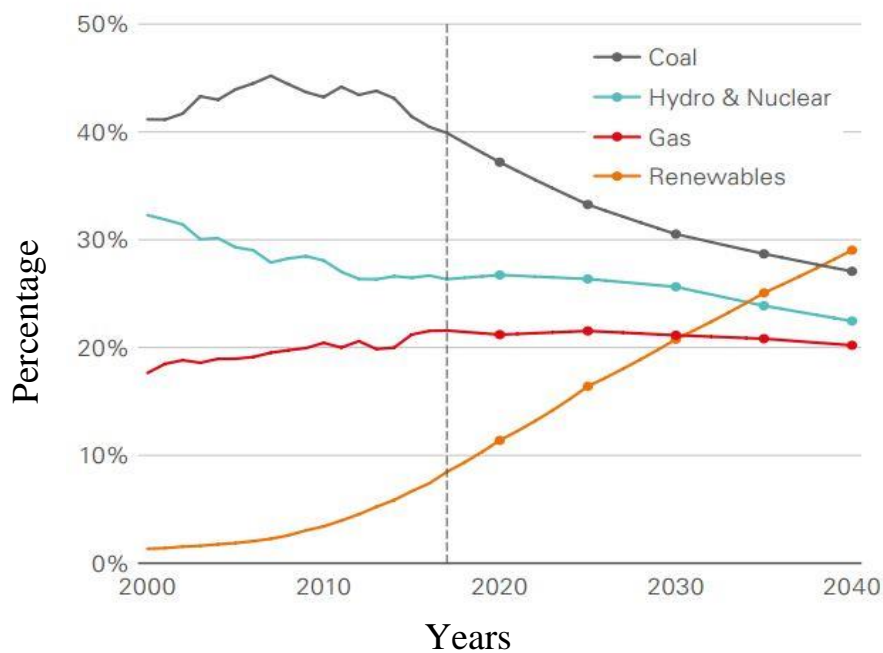


Fig1-1: Comparison of present trends of energy generation from different sources

Figure 1-1 represents the data for the fuel share mix of global energy production with respect to different generation sources. The growth rate of renewables is increasing every year and after 2010 it shoots up very strongly. At the end of this decade, Renewables accounts around two-thirds folds increment in power generation, with their share in the global power sector reaching level around 30%. Which ensures to reduce the burden on the coal for the additional demand. By seeing the growth trend, it is projected that by 2040 renewable will overtake coal as the largest source of global power[1]..

For the developing countries like India where population growth levels are rising over the years. Renewables can add extra bit of energy to existing conventional scale generation. So it become essential to harvest the inexhaustible resource of the nature. Besides the solar energy, other renewable energy technologies are developing at a faster rate. The wind energy has also been a successful alternative technology globally in order to produce electrical energy. Large wind turbines are installed in order to generate MW power. It has been found that the worldwide technical potential for wind energy is at second

after the solar energy. The biomass energy technology is also maturing day by day However, the solar energy is dominating the renewable market.

Table 1-1:Global Renewable Energy Potential (Exajoules Per Year)

| Source | Technical potential | Theoretical potential |
|-------------------|---------------------|-----------------------|
| Biomass Energy | >250 | 2900 |
| Solar Energy | >1600 | >39000000 |
| Wind Energy | 600 | 6000 |
| Small Hydropower | 50 | 150 |
| Geothermal Energy | 2.0 | 140000000 |

The data taken from Goldemberg, J. (ed) 2000. World Energy Assessment: Energy and the Challenge of Sustainability. New York: UNDP

. Sun is the ultimate source of energy. The earth surface receives over 120 000TW of sunlight, the vast majority of this energy cannot be harvested. In order to plan the electrical energy production, we need to assess the available potential of solar energy and proper technology and means have to be adopted for its full utilisation. Initially the solar energy is utilized in space applications only. But with rapid technological advancement over the coarse of years, the high efficiency and at the same time low cost devices were rapidly increased. This lead to widespread use of solar energy in terrestrial applications.

1.3 Solar Energy

Solar energy is referred to as the light radiant and the heat that is obtained from the sun by the people. It can be harnessed by using various technologies such as solar heating, photovoltaics, solar thermal energy, solar architecture and artificial photosynthesis. [2-3] Solar energy is considered as an important source of renewable energy and is mostly classified into active or passive solar depending on the means they use to capture and distribute solar energy to produce useful power. Active solar involves use of photovoltaics systems, concentrators, solar water heating system to harness energy. Passive solar energy techniques use sun orienting buildings, designing spaces for natural circulation of air.

1.3.1 Harvesting Technology

1.3.1.1 Solar Thermal technology:

In this technology the solar energy is converted into heat energy. Various ways have been used in order to generate as well as use the heat energy. In some case an absorber surface or a flat metallic surface can be used that will absorb the radiation from the sun and then transfer this heat to fluid like water or air as in flat

collectors of solar water heater. These collectors are simple in design and high temperature can be obtained by using suitable optics.

1.3.1.2 Photovoltaic systems:

The solar radiation can also be converted into electricity by photovoltaic effect as discovered by Edmund Becquerel, a French scientist in 1839. He found that solar energy consisted of photon which strikes on the solar cell and some of them are absorbed and electron hole pair generation occurs which are then separated in across the p-n junction resulting in a voltage across a junction which produces a current and then power is extracted. Therefore, these solar cells are also referred to as the photovoltaic devices.

To compare the two technologies, looking is in terms of diversifying use of the generated energy can be one way.

The Photovoltaic system has an advantage over other ways of harnessing energy technologies. In Photovoltaic the incident radiant is directly converted to Electricity. But in Solar thermal energy is captured in the form of Heat. Since Electricity is high grade energy and so utilization in different application can be done in more effective way. Heat is low grade energy and be used strictly for heat requirement. Because converting to electricity will lead further reduction of output in due to thermodynamic constraints.

1.4 Solar Cells

A solar cell is a p-n junction diode that is mostly used to convert solar energy into electricity based on photovoltaic effect. The solar energy incident on the surface in the form of photon. Then generation followed by the collection of the light generated carriers due to movement of electrons to the *n*-type side and holes to the *p*-type side of the junction. This transfer of charge carriers result in generation of current and voltage across the solar cell.[4].

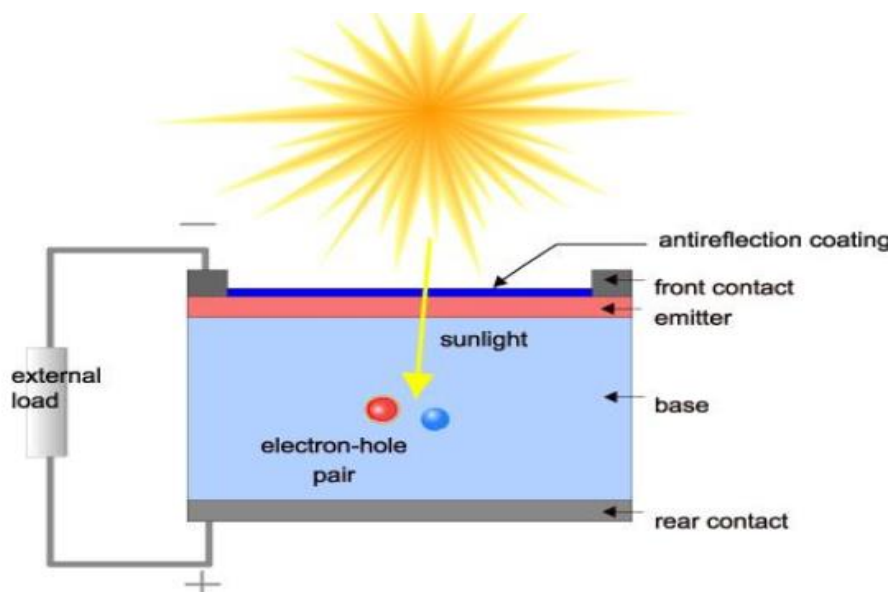


Fig 1-2: Construction of a solar cell

The various parameters on which the solar cell output characteristics depends on are :-

1.4.1 Short Circuit Current: (I_{sc})

It is the maximum current obtained when the p-n junction are in short circuit condition. The short-circuit current is due to the generation and collection of light-generated carriers. It depends on various factors

- 1 Area of the solar cell, so larger the area larger will be current
2. The number of photons, as the intensity of light increases the short circuit current also increases.
3. Collection Probability of solar cell that is the surface passivation and the minority carrier lifetime in the base.
4. diffusion lengths should be large as charge carriers generated within the diffusion length contribute to output current.

$$I_{sc} = qAG(Ln + Lp) \quad (1.1)$$

A=area of cell, G=Generation rate, L_n and L_p are the diffusion lengths on n and p side respectively.

1.4.2 Open Circuit Voltage (V_{oc})

It is the maximum voltage that is obtained at zero current or when the terminals are opened. The open circuit voltage is dependent on temperature. As the temperature increases V_{oc} decreases. V_{oc} is also strongly dependent on the saturation current of the solar cell and the light generated current

$$V_{oc} = \frac{nkT}{q} \left(\ln \frac{I}{I_o} + 1 \right) \quad (1.2)$$

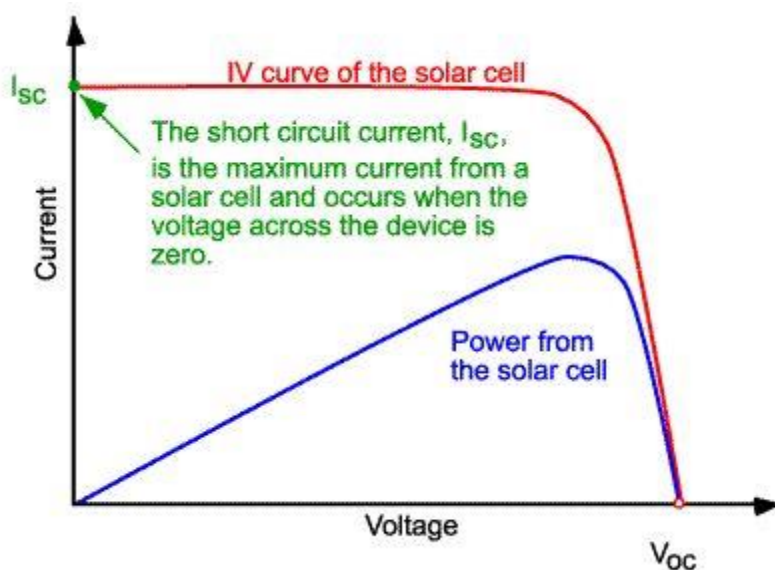


Fig 1-3: Curve showing I_{sc} V_{oc} and P_{max} from the solar cell.

n = diode ideality factor
 k = Boltzmann constant
 I = light generated current
 I_o = reverse saturation current

1.4.3 Fill Factor(FF)

The fill factor is defined as the ratio of maximum power from the solar cell to the product of V_{oc} and I_{sc} . The FF is a measure of squareness of I-V curve of the solar cell or the area of the largest rectangle which will fit in the I-V curve. Almost a solar cell with high voltage has a larger possible FF.

$$FF = \frac{V_{mp}I_{mp}}{V_{oc}I_{sc}} \quad (1.3)$$

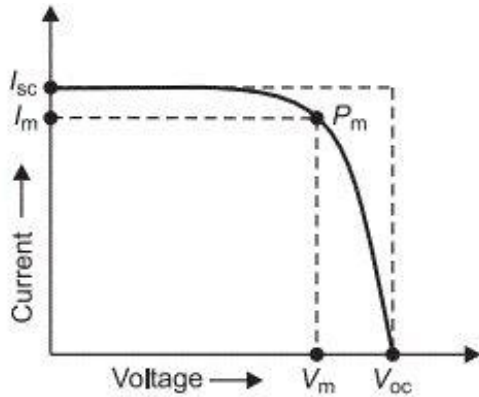
The terms V_{mp} and I_{mp} are the maximum voltage and current point in the I-V curve.

1.4.4 Efficiency

It is the most common parameter to compare the performance of one solar cell with another. It is the ratio of output electrical energy of solar cell with respect to incident radiation

$$\eta = \frac{V_{oc}I_{sc}FF}{P_{in}} \quad (1.4)$$

The efficiency of solar cell depends upon the spectrum and the intensity of incident sunlight as well as the temperature of solar cell.



The inner square represent the practical power extracted from the solar cell device.

The outer square represents the maximum possible output at two extreme conditions.

Fig 1-4 : Different voltage and current points in I-V curve

The above mentioned parameters collectively defines the electrical output of the solar cell. Apart from these, the parameters to compare under specified test condition called as Standard Test Conditions(STC). This test conditions is 1000W/m^2 intensity with temperature 25°C and AM1.5 These conditions vary a lot when worked in the field. The maximum theoretical efficiency defined by Schokley-Queisser is upper thermodynamic limit for a single electron-hole pair generation by photovoltaic effect. Losses are the main reasons that limits the performance of Solar Cell. So a study of loss mechanism is essential to reduce them.

1.5 Losses in Solar Cell

The performance is strongly affected by different kinds of losses throughout the solar cell. There are usually two types of losses occur in a solar cell mainly fundamental losses and technological losses. The fundamental losses involve excess and low photon energy, and these conditions are unavoidable. The technological losses include optical and electronic and electrical losses that can be solved by various technological advancement.

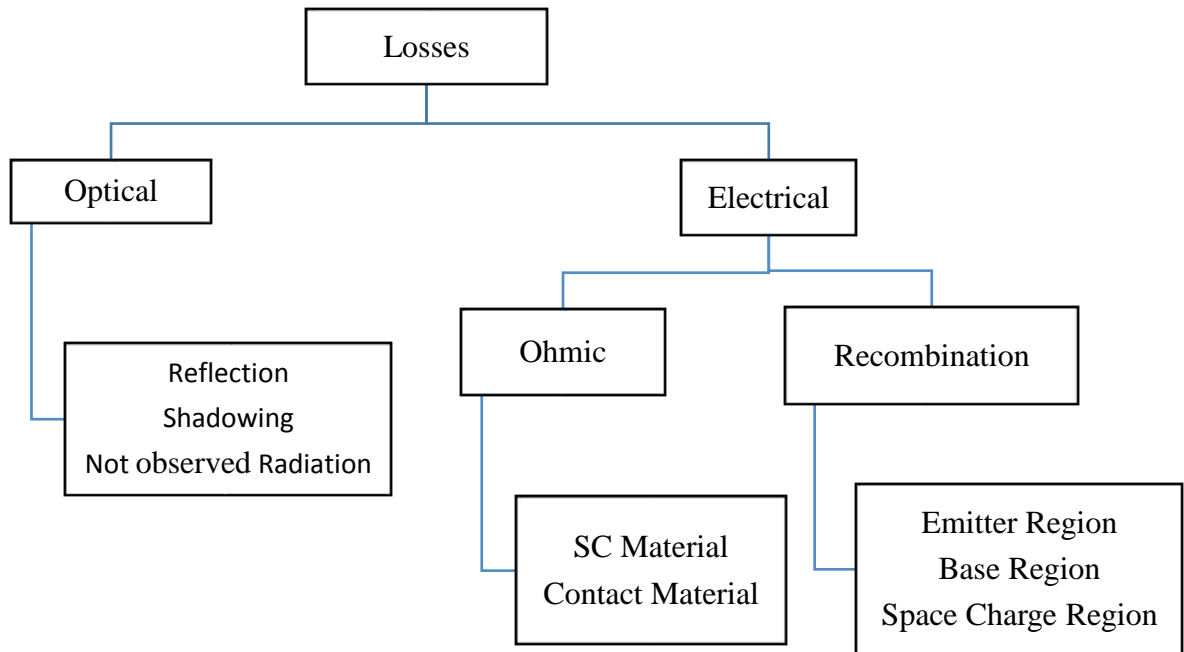


Fig 1-5: Summary of losses occur in a solar cell

1.5.1 Optical Losses

These come into picture when light which could have generated an electron-hole pair but couldn't because the light may get reflected from the front surface, or because it might not get absorbed in the solar cell.[5] The optical losses mostly involve unabsorbed solar radiation reflection and can be reduced by several ways :-

1. Anti-Reflection coating on the top of solar cell.
2. Surface texturization to reduce reflection.
3. Minimizing top contact coverage to reduce contact shading, series resistance.
4. Thickness reduction of solar cell to increase absorption of low energy photons.

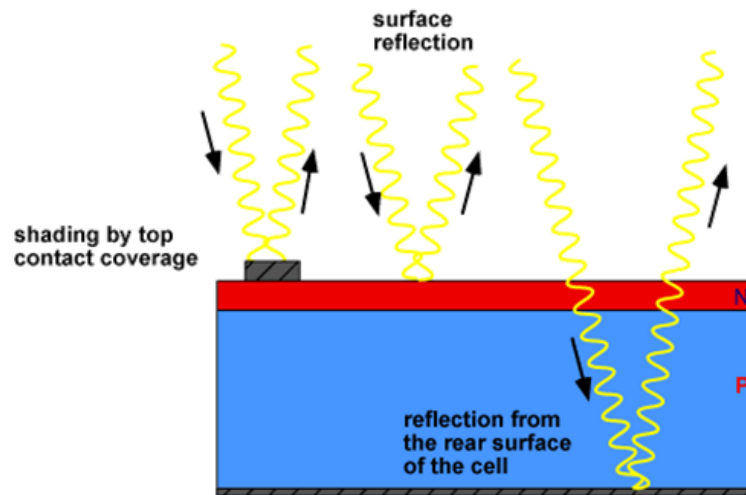


Fig 1-6: Reflection Losses at the surface,

1.5.2 Electrical Losses

1.5.2.1 Ohmic Losses

The ohmic losses arrive due to series resistance effect. Series resistance in the device arrives due to the firing of metal contacts with the cell. The series resistance includes the combined resistance offered by the emitter, bulk, and the space charge region. The current collection at the end terminals is greatly reduced if this parameter value is high. Similarly, the shunt resistances arrive when there is some leakage path through the cell. Essentially, for a good solar cell, R_{series} and R_{shunt} should be low and high respectively.

1.5.2.2 Recombination Losses

Generation and Recombination are the basic phenomena that occur in a solar cell. Hence, one cannot eliminate recombination completely. The loss of carriers would result in the release of energy in the form of either photons (lattice vibrations) and phonons. The existence of defects over the cell are the main cause behind this. Recombination losses affect both current collection, i.e., short circuit current as well as open circuit voltage. There are three basic mechanisms of recombination, that are listed below:

1. Radiative Recombination
2. Shockley–Read–Hall Recombination
3. Auger Recombination

SRH and Auger Recombination are major mechanisms that happen in a silicon solar cell. Silicon is an indirect band gap semiconductor. Recombination is classified according to the region of the cell in which it occurs. So, therefore, the bulk and the surface are the main regions [6].

In order to reduce the surface recombination it mainly aims on reducing the number of dangling silicon bonds that are present at the top surface by means of passivating layers. In a commercial solar cell dielectric layers such as Silicon Nitride or hydrogenated Silicon Nitride are commonly used.

To quantify surface recombination the term Surface Recombination Velocity is one way. Surface recombination velocity (SRV) is used to represent the flux of the carriers towards the surface of the semiconductor. Being a surface phenomenon, the unit of surface recombination in cm^2 . Lower the flux of minority carriers towards the interface, lesser is the recombination, and hence lesser the value of SRV..

Recombination of charges is measured in terms of Surface Recombination velocity (SRV) and carrier lifetime (τ_{eff}). There are two possible ways of reducing the SRV

1. It can be lowered by reducing the number of interface trap density associated at the surface. This logic forms the basis of chemical passivation, where the dangling bonds existed due to abrupt termination of crystal structure are terminated by hydrogen or by growing any thermal oxide layer.
2. Another scheme include lowering the surface concentration of any one type of charge carriers like ps or ns, the surface electron and hole concentration density can reduce the rate of recombination and. This logic forms the basis of field effect passivation. It can be done following ways (a) by externally adding layer whose doping profile is such that it could repel the minority carriers towards the bulk. (b) or by application of external voltage source to repel the minority carriers away from the interface. (c) by the help of charges in the dielectric existed at interface to force the minority carriers away from interface.[7].

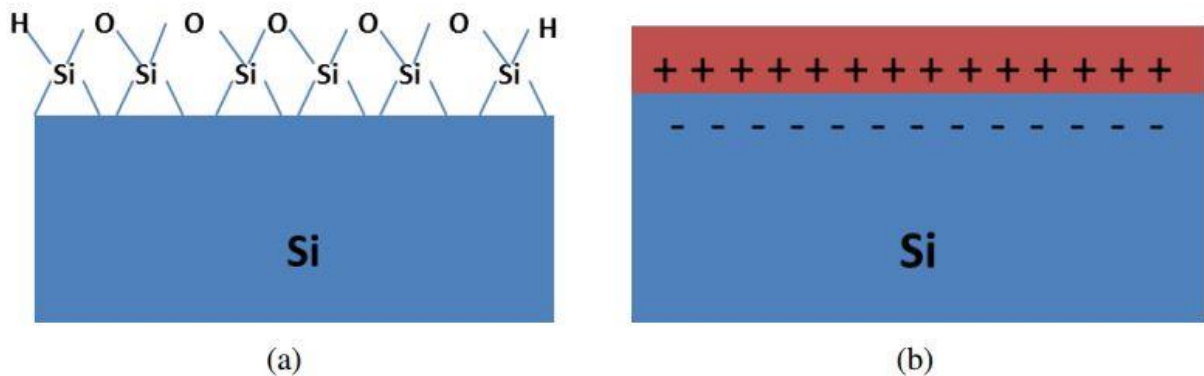


Fig:1-7 Representation of two types of passivation scheme (a) chemical passivation (b) field effect passivation

. SRV is measured from the lifetime measured in a lifetime tester using the following equation.

$$\frac{1}{\tau_{\text{bulk}}} = \frac{1}{\tau_{\text{rad}}} + \frac{1}{\tau_{\text{Aug}}} + \frac{1}{\tau_{\text{SRH}}} \quad (1.5)$$

Here, τ , t_{bulk} is the bulk lifetime, τ_{rad} is of radiative lifetime, τ_{aug} is auger lifetime and τ_{SRH} is Shockley Read Hall Lifetime.

1.6 Transition Metal Nitrides

The family of Transition Metal nitride include Titanium Nitride (TiN), Zirconium Nitride (ZrN), Chromium Nitride (CrN), Vanadium Nitride (VN), Niobium Nitride (NbN), Tantalum Nitride (TaN) and Tungsten Nitride (WN) and so on. Each of these will have varying properties and microstructure depending on the type of deposition process. Due to their superior mechanical properties ,conventional application of these nitrides include corrosion and wear resistant coatings[8].Their usage has impacted wide variety of application that are used for microelectronic industry , solar collectors , engineered coatings along with optical and tribological coating .It is due to unique physical and chemical properties, among them some are wear resistance, good adhesion and chemical stability[9]. Their high thermodynamic stability with very high melting point (around 1500C) and electrical properties that open up potential application as protection layer used in fission reactors.[10]

Normally transition metal nitrides are yellow, brown and gray in color with face centered cubic structure. Titanium nitride thin film is taken under investigation. In transition metal nitrides, like Titanium Nitride (TiN) is among one of the important materials, used as protective coatings, high hardness, wear resistance , corrosion resistance and thermal stability[11]. Titanium nitride thin films have been serving the scientific industry over a wide genre of application for more than 20 years. The optimization of coating structure can provide significant improvement in mechanical, optical and electrical properties of the coating . It has also serves as anti -reflective coating and also as diffusion barrier in the microelectronic industry[15] . Titanium Nitride films have been used as decorative for cosmetic artificial gold surfaces, and its optical characteristics has made it useful for selectively transparent films like(‘heat mirrors’), solar absorbers for high temperature use, and energy-saving window coatings [12]. It also posses advantageous optical properties and metallic conductivity. Titanium is a light metal

It is found in the study that Stoichiometric TiN is a good conductor of electricity in its crystalline form whereas TiN is a very good insulator in amorphous form or nitrogen deficient (sub-stoichiometric) . Both amorphous and sub-stoichiometric TiN film exhibits high transmission of light in the visible region and also high electrical resistivity[13] One of the main factors that forms the basis is the deviation of physical properties of TiN thin films from those of the bulk is the presence of sub-stoichiometric impurities. With the change in nitrogen fraction and impurities as like oxygen affects the properties of TiN thin film. Controlling oxygen content is essential, as the free energy of formation for titanium oxides is much lower compare to TiN which leads to undesirable titanium oxides traces even with a small amount of oxygen

present. The colour of TiN also varies strongly with change in composition. Increasing nitrogen content in the film leads to the color changes from a titanium grey to light yellow (Ti_2N) to golden (TiN) to brown to bronze, and finally red [14], with the presence of H_2O or O_2 adding a purple hue.

In this study, TiN thin film – semiconductor MIS device structure is required to analyse the types of defects.. Engineering of interface study of Metal – Semiconductor and Dielectric- Semiconductor plays essential role in device scaling aspects. The parameters associated with it provide an understanding of carrier dynamics inside the Metal Oxide Semiconductor. Oxides layer prepared for very low thickness are prone to higher leakage currents and can have pronounced effects on device characteristics. Defects during the fabrication is also an important parameter

1.7 Metal Insulated Semiconductor(MIS) Structure

To study the properties of semiconducting surface, the metal-insulated semiconductor(MIS) capacitor is most useful device. Practical problems of semiconductor devices properties are closely related to surface phenomenon. Hence an understanding of surface physics are realized with the help of MIS capacitors. It is essential a combination of metal, insulator or dielectric layer and the semiconductor sandwiched together.[16]

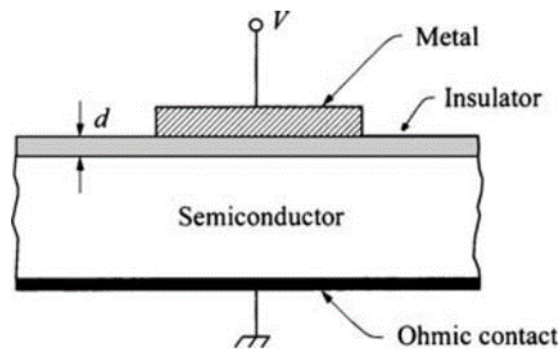


Fig 1-8: Metal Insulator semiconductor in cross section view.

where d is the thickness of the insulator and V is the applied voltage.

An ideal MIS is defined by two conditions:

1. The only charges exist in the structure under any biasing conditions are those in the semiconductor and those, with an equal but opposite sign, on the metal surface adjacent to the insulator, i.e., there must not be any interface trap nor any kind of charge;
2. There is no carrier transport through the insulator under dc biasing conditions or the resistivity of the insulator is infinite.[16]

1.7.1 C-V Characteristics of a MIS device

The capacitance voltage characteristics of MIS device can provide lots of derived quantities like flat band voltage, threshold voltage, effective charge density and interface defect density. The basics of capacitance voltage measurements of MOS device is divide into three regions. -

For a p-type substrate, the regions are attained as per the nature of polarity applied at the gate bias. Fig 1-10 shows the typical C-V curve under different frequency

Accumulation : Pile up of majority charge carriers at the interface due to applied negative voltage at gate,

Depletion : Removal of majority charge carriers at the interface, as the bias value shifted towards positive voltage values.

Inversion :Pile up of minority charge carriers at the interface, as the bias value starts from negative gate bias voltage values. Depending upon the magnitude of reverse polarity voltage the inversion broken down into weak inversion and strong inversion..

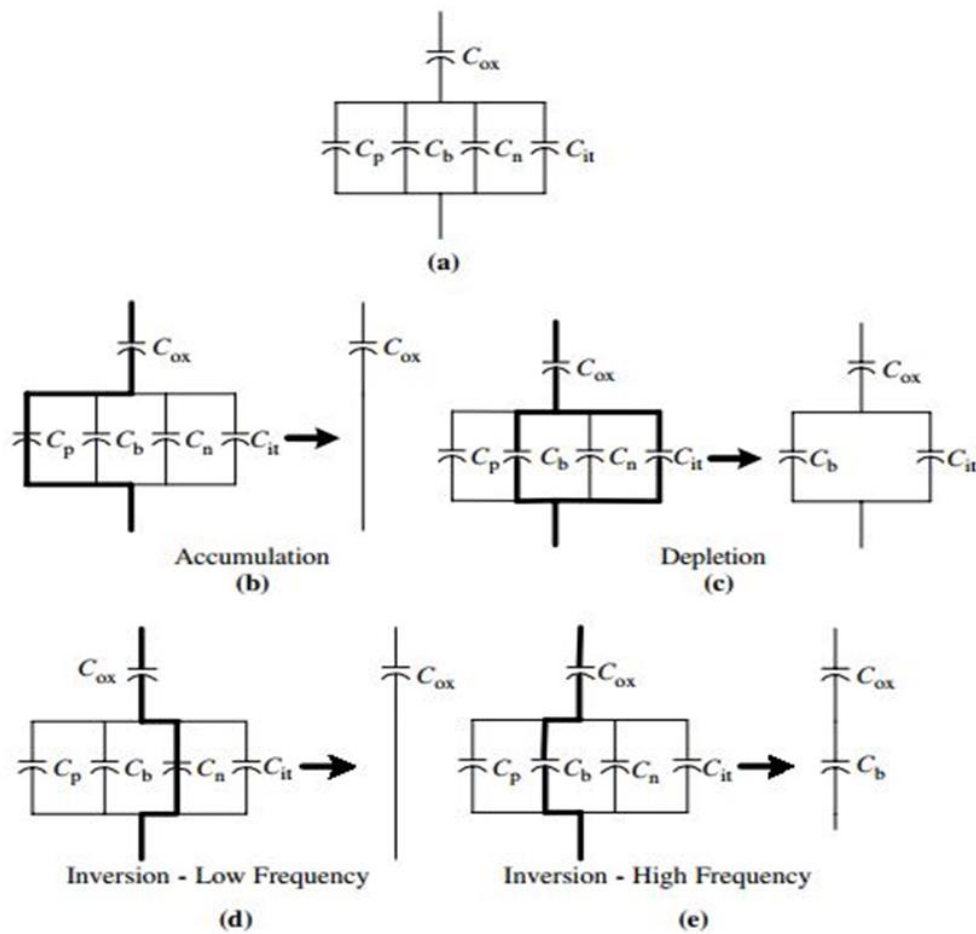


Fig 1-9: Capacitance of a MOS capacitor under various bias condition (a) Equivalent MOS device in terms of capacitance. Capacitance as seen in (b) accumulation regime (c) depletion regime (d) Inversion Low frequency (e) Inversion High frequency.

During sweep from accumulation to Inversion various types of capacitance appears which in turn effect the net capacitance value. For a p-type silicon as substrate the bias is applied to see its characteristics, Let us start from negative gate voltages, the surface gets heavily accumulated with majority carriers holes, C_p dominates over the other semiconductor capacitance. Thus resulting in C_p capacitance in series with C_{ox} capacitance, series combination of C_{ox} and C_p will result only C_{ox} in accumulation and assume C_p be short circuit. When the gate voltage is moved towards zero and further in the positive direction, the surface becomes more and more depleted, the space charge region density Q_b and so correspondingly C_b dominates also trapped interface charge capacitance also contributes. So the bulk capacitance C_b of the space charge region comes in parallel to the interface capacitance C_{it} also comes in the picture. Now the total capacitance is the combination of C_{ox} in series with C_b in parallel with C_{it} . As the gate voltage is further increased in the positive direction, the surface starts getting inverted At this point, the inversion capacitance depends on the frequency of the small signal ac voltage applied along with the DC one , the small signal ac voltage drives the device periodically above and below the fermi level. At low frequency ac gate voltage, the minority electrons are able to follow the periodic variation with gate voltage , this is case of weak inversion so C_n begins to dominate and resulting C_{ox} again in series combination thus low frequency C-V is measured which in series combination becomes oxide capacitance again.. On the other hand, for high frequency ac gate voltage (10 kHz- 1 MHz),the minority carriers (here electrons) are unable to follow the fast variation of ac gate voltage and therefore, the applied gate signal is balanced by increased space charge bulk capacitance C_b and high frequency C-V curve is measured [17].

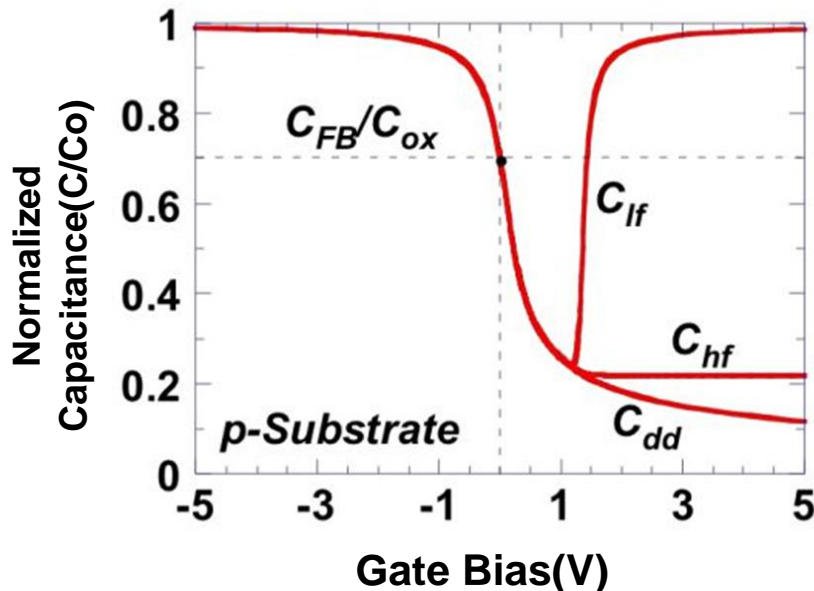


Fig 1-10: Normalized Capacitance Vs. gate voltage for low frequency and high frequency

1.7.2 Defects

There are basically four types of charges associated with the Silicon and dielectric system as shown in fig. In each of the charges following measurable quantity starting from Q is the net effective charge per unit area at the dielectric-silicon interface (C/cm^2), N is the net effective number of charges per unit area at the interface ($number/cm^2$), also D_{it} , which is given in units of $number/cm^2.eV$.

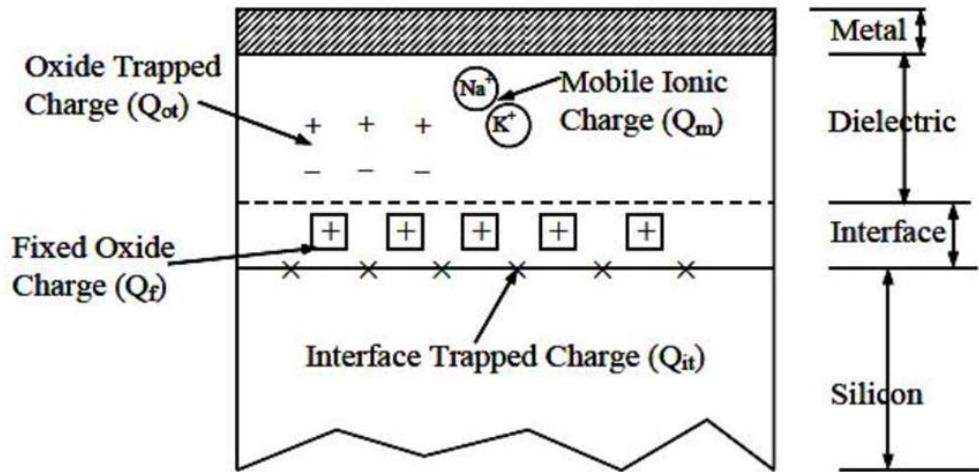


Fig 1-11: Different types of defects exist in MIS Device

1. **Interface Trapped Charges (Q_{it} , D_{it})** : These are the positive and negative charges that arrive from structural defects, metal impurities or other defects such as abrupt termination of the crystalline Si lattice, incomplete bonds and absorption of foreign material at the silicon surface. The trap charges are located at the dielectric-semiconductor interface. These type of charges have electrical communication with the underlying silicon.[17]
2. **Fixed Oxide Charge (Q_f)** : As per the conventional definition with respect to Si-SiO₂ interface. This charge density has its origin related to the oxidation process, that in turn depends on conditions of oxidation ambient and temperature, cooling conditions. Unlike the interface trapped charges, the fixed charge does not have any electrical connections with the underlying silicon. These charges are dependent upon silicon orientation and annealing conditions but are not affected by thickness and semiconductor doping levels.[17]
3. **Oxide Trapped Charges (Q_{ot})** : It can be seen as electrically neutral sites that are distributed throughout the oxide (or in our case dielectric). These sites can be easily charged with introduction of electron or holes. These charges may be positive or negative that depends whether the holes or electrons are trapped in bulk of the oxide. [18]
4. **Mobile Oxide Charge (Q_m)** : This is caused primarily by alkali ions such as Na⁺, Li⁺, K⁺ etc. that are unwanted impurities that get attached during device fabrication. Unlike the trapped and fixed charge which

are localized at a specific site but they can move about within the oxide(or dielectric). This position dependence is the basis of what is called the bias-temperature stress test for measuring the mobile ion content, Q_m . [18].

1.7.3 Effect of sweep direction in the C-V curve

For C-V measurement, the applied gate voltage must be superimposed with the small signal ac voltage. As far as frequency dependence in the C-V curve they are almost identical in accumulation and depletion. The curves deviate from one another when the device enters inversion. The frequency of applied small ac voltage is termed as ac probe frequency. For a slow dc voltage sweep, inversion charge to form if the ac probe frequency is of a sufficiently low frequency for the inversion charge to be able to respond to that, then the low-frequency curve is obtained. Whereas if the ac probe frequency is too high for the inversion charge to be able to respond, then the high-frequency curve is obtained for the slow dc voltage sweep

If the bias is swept from accumulation to inversion region, there will be tendency of C-V curve to go into partial deep depletion and the curve will go below the actual curve as shown in fig 1-10

The true curve is obtained when after a set bias voltage, allowed to relaxed for a while for the device comes under equilibrium, then repeating it point by point to generate the C-V curve. This is beneficial as the charges will be getting sufficient time to come under normal state. The preferred direction is from +V to -V sweep direction, since the deviation from the true value is less from the other direction sweep from -V to +V in case of p type substrate [17].

From the above paragraph, an inference is drawn to sweep from inversion to accumulation. And hence if dealing with n-type substrate the preferred direction will be opposite that is from -V to +V.

1.7.4 Conductance Method

Conductance method is a way which we replace MIS capacitor with equivalent circuit models and calculate interface defect density (D_{it}). The conductance method is particularly powerful because the measured quantity, the MIS parallel conductance, generally relates directly and solely to the interface states. This is not the case for capacitance-based methods, where the measured capacitance contains contributions from the semiconductor and dielectric which must be separated from that of the interface states.

1.8 Aim of the present Work

In the earlier section, it is shown that Titanium Nitride thin film has wide range of application in different areas. Though its potential is not fully realized with Silicon Solar Cells. Its optical properties like high

transparency and wide band gap can be one advantage to allow maximum absorption. With better mechanical properties, it may provide additional strength. Since it is traditionally utilized as a diffusion barrier in microelectronics so this feature can be extended to solar cell to protect from sodium ions impurity from the top (glass).

In order to have such properties, it is important to derive the optimized condition to prepare titanium nitride thin film. Sputtering is a physical vapour deposition process of creating thin films over the substrate. Since it is relatively simpler than other complicated processes like Atomic Layer Deposition (ALD) etc and can be an industrially scalable process. One can get produce thin film at low cost and at a large scale. The aim of the project can be divided into four parts.

1. The first objective is to see the variation of film transparency on the glass slides with changes in Nitrogen flow rate and Argon Flow rate. The variation in flow might create film of different stoichiometry
2. To build a MIS device by deposition over silicon substrate to see its electrical parameters and defects. After that to passivate the surface by Hydrogen at lower temperatures to reduce defects. Thus transparency, defects and passivation effect is measured with respect to flow rate.
3. To see the effects of thickness variation in the film the deposition time is changed and similar comparison with transparency, defects and passivation effect is performed. An optimized condition is achieved
4. The optimized condition is deposited over the Silicon solar cells. The current voltage characteristics and EQE measurement is performed to compare the results with planar silicon solar cells with that of titanium nitride film deposited over silicon solar cells.

CHAPTER-2

Thin film deposition processes and Characterization Techniques

2.1 Thin Film Deposition Process

2.1.1 Introduction

People around the globe are looking forward towards novel material which has extraordinary combination of physical, chemical and mechanical properties. Thin film technology has greatly impacted the solid state electronics. It may possibly started with the observation of Grove, when he found that metal films were formed by sputtering of cathode with high energy positive ions [19]. Thomas Edison was apparently one of the first to use for a product by applying a thin layer of metal to the outside of his wax phonograph recordings in 1904[20]. Early attempt in thin film deposition include the research conducted by Michael Faraday in 1857. In the series of experiments, Faraday created thin metallic films by exploding metal wires in a vacuum vessel [21]. Thin film is generally referred as materials having effective 2-dimensional form by limiting one of the physical dimension that is thickness not greater than few micro meter by a growth process. Due to geometry, dimensional constraint and microstructure that are characterized by non-equilibrium growth process, thin film shows unique property compared to corresponding bulk. It is basically thin layer of coating of material over the bulk substrate that have magnitude ranging from few hundred angstrom(ultra thin) to few nanometres (thick films). The characteristics of thin film can be tailored to obtain many physical properties like electrical, thermal, mechanical properties of the combined systems. Table 2.1 divides thin film properties into five basic categories with typical applications within each category [19].

Table 2-1: Thin film property and its respective application

| Thin Film Property Category | Typical applications |
|-----------------------------|--|
| Optical | Optical memory discs(CD's, DVD's) Decorations (color, lusture) Reflective/antireflective coating |
| Magnetic | Memory discs(Hard discs and tapes) |
| Electrical | Conduction Insulation Semiconductor Devices Piezoelectric drivers |

| | |
|------------|--|
| Thermal | Heat Sinks Barrier Layers |
| Mechanical | Hardness Tribological (wear-resistant) coatings |

Such low thickness as a dimensional constraint cause tremendous increase in the surface area to volume ratio and so the surface properties of the material dominate over the bulk in thin film region. In a growth process, the incorporation of defects may provide different microstructure which could be manifest in unique properties, for example- increase in the resistivity of the film. The classification of thick and thin film are often done on the basis of usage and application. Like if the film is used for the surface properties (like catalytic activity, reflectivity) then it is referred as 'thin film' else if it used for its bulk properties like erosion, wear and corrosion resistance, it is referred as 'thick film' [22] or coating, which is the surface engineering terminology for thick film.

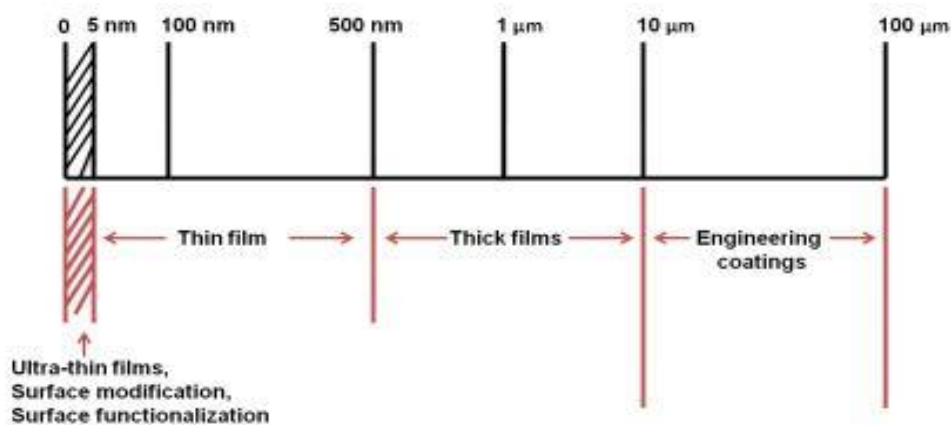


Fig 2-1: Thin and thick film regimes

The usefulness of the optical properties of metal films, and scientific curiosity about the behaviour of two-dimensional solids has been responsible for the immense interest in the study of science and technology of the thin films. Thin Film Deposition technology can be regarded as the major key to the creation of devices such as computers, since microelectronic solid-state devices are all based on material structures created by the deposition techniques.

2.1.2 Thin Film Deposition techniques

Deposition process play essential role in defining the characteristics of thin film. With different deposition techniques , a proper tailoring of the micro and nano-structure of the layers can be achieved. These process provide enormous flexibility that allows the growth in desired physical, topographical, geometrical,

crystallographic and metallurgical in lesser dimensions .For any deposition method there are basically three distinct steps that are followed to deposit thin films:-

1. Production of the appropriate constituents of atomic, molecular or ionic species.
2. Transport of these species to a suitable substrate through vacuum or a suitable fluid medium.
3. Deposition onto the substrate via direct condensation or chemical/electrochemical reaction and subsequent film growth.

The process by which materials interacts with the substrate plays an important role in defining the various ways of depositing thin film. Deposition techniques can be broadly classified into two different ways :-

1. Chemical Vapour Deposition
2. Physical Vapour Deposition

2.1.2.1 Chemical Vapour Deposition (CVD):

Chemical vapour deposition is a growth method in which the constituents of vapour phase react together to form a solid film at the surface. Deposition takes place due to a chemical reaction between some reactants on the substrate Here reactant gases (vapours of precursors) are pumped in to a reaction chamber The chemical reaction is initiated at right conditions of temperature and pressure near the substrate surface which leads to the desired material in the form of a deposit on the substrate. The reaction may produce by product that are pumped out. The key parameters for the chemical reaction rates are gas transport, diffusion etc. By changing the experimental conditions, like substrate temperature, composition of reaction gas mixtures, total pressure gas flows may yield to different properties of grown film. The chemical reaction is the characteristics of this kind of deposition method, The morphology, microstructure and adhesion of the deposited film are strongly influenced by the nature of chemical reaction and the activation process [23]. The are wide range of methods that fall under this category :-

1. Atmospheric Pressure Chemical Vapour Deposition (APCVD)
2. Low Pressure Chemical Vapour Deposition.(LPCVD)
3. Atomic Layer Deposition (ALD)
4. Sol-gel Method
5. Hot- Wire Chemical Vapour Deposition.(HWCVD).

Besides above listed techniques there are various other methods of chemical vapour deposition

2.1.2.2 Physical Vapour Deposition (PVD)

In physical deposition technique, mechanical or electromechanical methods are used to deposit the thin films on the substrate. Materials to be deposited on the substrate depend upon the temperature, pressure and other physical conditions. In these physical methods, the thin films formed are directional on nature because particles will follow a straight path from the target to the substrate. It is fundamentally a vaporizing coating process in which the basic mechanism is an atom by atom transfer of material from the solid phase to the vapor phase and back to the solid phase, or gradually building a film on the surface to be coated.[24]. The vaporized material receives the energy from external environment and when it faces the cool substrate surfaces, it draws energy from these particles as they arrive, allowing them to form a solid layer. In the case of reactive deposition, the depositing material reacts with a gaseous environment of co deposited material to form a film of compound material, such as a nitride, oxide, carbide or carbonitride. Aluminium, Gold, Silver, Titanium and other metals are commonly used materials that are deposited using this Physical Vapour Deposition. All film deposition occurs under vacuum or very carefully controlled atmosphere.

The different level of vacuums corresponding to pressure ranges.

| | |
|-------------------|-----------------------------|
| Rough Vacuum | 1 bar to 10^{-2} mbar |
| High Vacuum | 10^{-3} to 10^{-6} mbar |
| Very high Vacuum | 10^{-6} to 10^{-9} mbar |
| Ultra-high Vacuum | $< 10^{-9}$ mbar |

Physical Deposition technique include the following methods :-

2.1.2.2.1 Evaporation

In the process of evaporation, heat is transferred into the source material (often called the charge, which may be an elemental metal, an alloy, a mixture or a compound) to create a plume of vapor which travels in straight line paths to the substrate. The atoms, molecules, and clusters of molecules condense from the vapour phase to form a solid film, upon arrival at the substrate. The heat of condensation is absorbed by the substrate.[25] In the process of evaporation techniques, different ways are utilized to apply heat to the source.

2.1.2.2.1.1 Thermal Evaporation

Thermal evaporation is a common method of thin-film deposition. It is used for depositing metals and some compounds with low melting temperature. First, the source material is evaporated in a vacuum. The vacuum allows vapour particles to travel directly to the target object (substrate), where they condense back to a solid

state. In thermal evaporation resistive coil or boat is used that contains charge in solid bar or powder form. A large DC current passed through resistive coil/boat to acquire high melting points of respective metals, where metal get evaporated and attain to substrate in high vacuum conditions. Vacuum conditions ensure no contaminations. The thermal evaporation chamber can be evacuated using a diffusion pump to create high vacuum levels. The material that is to be deposited is placed in heater or the crucible that is heated by DC power supply. In high vacuum (with a long mean free path), evaporated particles can travel directly to the deposition target without colliding with the background gas. Hot objects in the evaporation chamber, such as heating filaments, produce unwanted vapours that limit the quality of the vacuum.

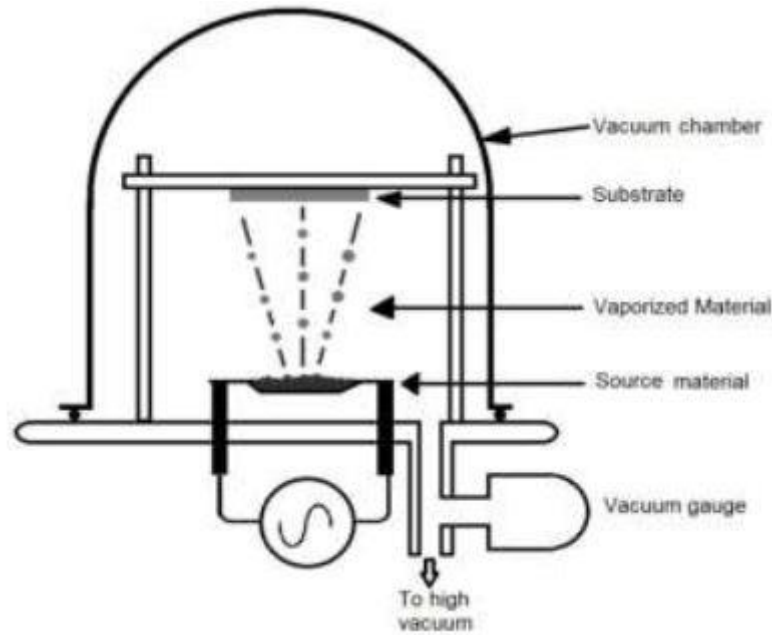


Fig2-2: Schematic showing thermal evaporation

2.1.2.2.1.2 The Electron beam technique

This method uses the intense beam of high energy electrons to evaporate source materials. The electron beam is generated by an electron gun assembly, which uses the thermionic emission of electrons produced by an incandescent filament. Emitted electrons are accelerated by a high voltage potential (kilovolts) into a source material can generate enough energy density to evaporate material. The combined force, F , on an electron in electric (E) and magnetic field is known as the Lorentz force and is given by :-

$$F = F_E + F_B = q_E + q_E (v \times B) \quad (2.1)$$

Where, F is in newtons/ m^2 , q_E in coulombs, E in V/m , B in $webers/m^2 = Tesla$, and the electron velocity v is in m/s . The first force term in equation, accelerates the electrons away from the cathode. As per the second force term, the velocity v so acquired causes the electrons to be deflected sideways as they cross the magnetic field lines. This second force is balanced by the centrifugal force of the electrons moving at radius r . the beam should be aimed at the centre of the source material and to avoid hitting the material's container

(Hearth) .The electrons emitted from the heated cathode are caused to travel in an oval shaped path by the electrostatic negative field applied to the cylindrical focusing electrode. A strong magnetic field bends the beam through 270 °C causing it to be incident on the surface of the material. The beam can be rastered across the charge to melt a significant fraction of the surface. The hot portion of the charge is then effectively self-contained by the cooler portion of the charge. Water cooling is provided thermally to the bottom of the charge. The source material is usually contained by a boat in the “hearth” which is water cooled to prevent its outgassing or melting. Cooling also prevents the hearth from alloying with molten source materials, because the material immediately adjacent to a cooled hearth cannot melt. It provide additional advantage as it can offer convenient way to have multiple sources in the evaporator, even if only one of them is to be used at a time. Such an arrangement allows deposition of different materials without opening the high vacuum chamber.

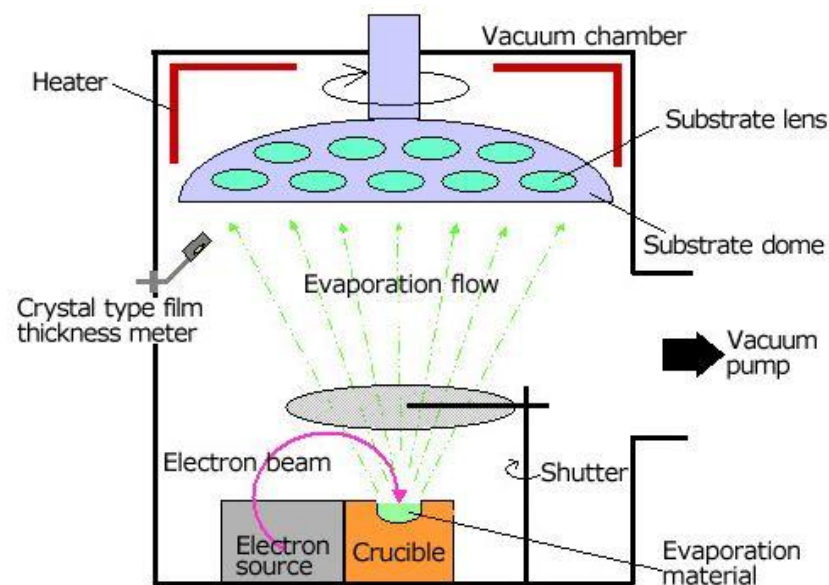


Fig 2-3 : Mechanism for e-beam evaporation .

In this dissertation work, sputtering technique has been used to deposit TiN layers, so in the rest of the chapter sputtering process will be explained in more elaborate fashion.

2.1.3 Sputtering

In general, sputter means to knock out particle from surface of material by means of collision. It is based on momentum exchange principle. It is useful for materials, which are not easily evaporated. It is a process of ejection of atoms from the surface of a target material by bombardment with high energetic particles. It is done by first creating gaseous plasma and then ions are accelerated from this plasma to the source material. The material undergoes continuous erosion by the arriving ions particles by energy transfer followed by ejection in the form of neutral particles like single atom or cluster of atoms or can be molecule.

These ejected source particles will travel in straight line till it comes contact with some other particles or surface. If the substrate like microscopic glass or silicon is placed between the path, then a thin layer of source material gets deposited on the substrate.

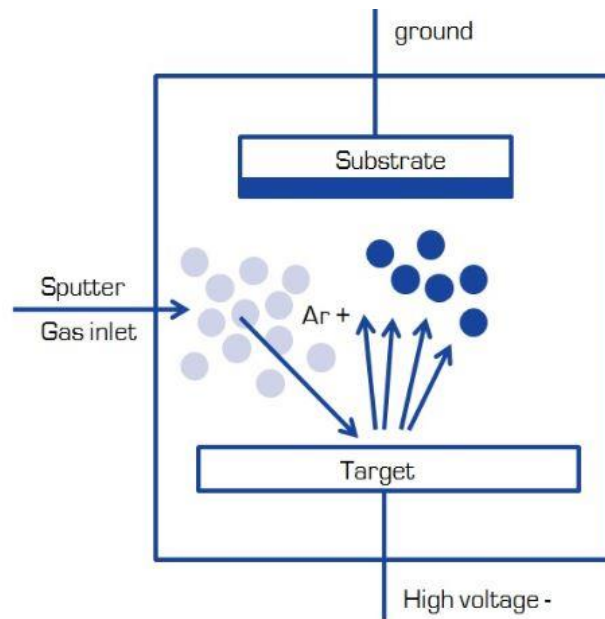


Fig 2-4: Schematic of sputtering process

2.1.3.1 Mechanism of Sputtering

Power supply is connected in such a way that negative potential is applied to the source material which is to be sputtered. Electrode connected to target acts as cathode and the chamber body is grounded. This electric field initiates the sputtering, the first collision occurs between free electron at target surface and the incoming gas atom, it results in displacement of electron from the gas atom and creates a positively charged ion (Ar^+ or any other noble gas). The positively charged ions then rushes towards the target surface due to polarity. The energy that it attains is enough to knock off sputter some of target material which follows and get stuck at the other end i.e substrate facing towards the target. A plasma glow is created when the ions recombine with free electron at lower energy state. The recombination with an ion, it has a specific voltage but the ion needs relatively less voltage. So this excess voltage is let off as light or plasma. The light is called as plasma glow or glow discharge process.

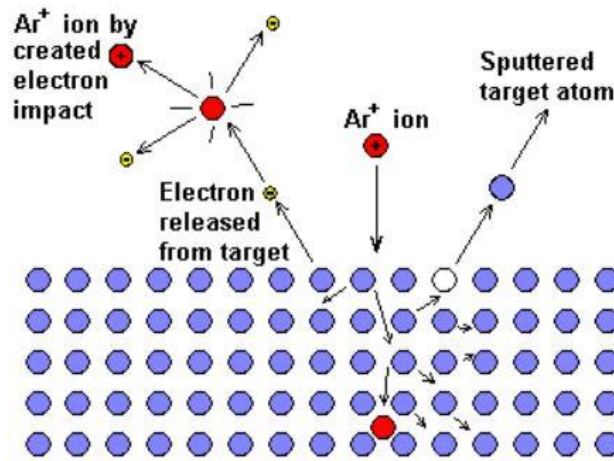


Fig 2-5: Mechanism of particle interactions at the target

Advantage of Sputter Deposition

1. Elements, compound and alloys can be sputtered and deposited.
2. The sputtering target provide a long-lived, stable source of desired material to be deposited.
3. Reactive deposition can be accomplished with the help of reactive gaseous species that forms compound in the activated plasma.

2.1.3.2 Advantage of Sputtering over other Methods.

In sputtering, the entire surface area of the target is considered as source, unlike the other PVD process such as e beam evaporation process where a point (where electron beam hits) is source. Some of the main advantages of sputtering is due to high kinetic energy of the sputtered atoms, that causes a re-distribution over the substrate surface, This provides (a) high uniformity, density and interface roughness of the deposited film (b) deposition over large surface area. Sputtering process can be further divided into three categories :-

1. DC/RF Sputtering

Depending upon the type of source used to energize the ions, the process is classified as DC or RF sputtering. The applicability of type of source used depend whether the target material is metallic or insulator. DC sputtering is used for metallic targets like Titanium. DC source is not feasible for insulators, because the ions that hits the surface their charge will remain localized and with passage of time positive charge will build up on the target, making it unfeasible to further bombard the surface. This limitation is removed by RF source by hitting the target by electron and positive ions simultaneously. The RF source provides energy to the electrons makes them to oscillate in the alternating field that initiates ionizing collisions. Since electron has high mobility than ions, there is increased number of electron reaching the

insulating target material in positive half cycle. This cause target to be self negatively biased. This leads to formation of sheath constituent of more positive ions at the front surface of target.[chapter 2 : Thin film]
An industrial standard of RF source of value 13.36 MHz for sputtering is set.

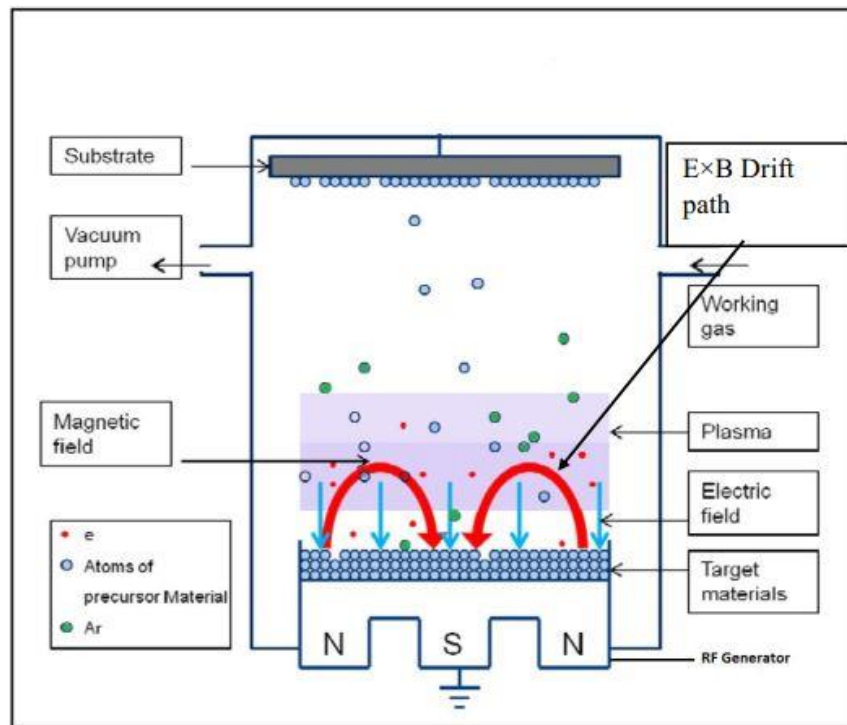


Fig 2-6 : Schematic of mechanism of RF sputtering

2. Reactive Sputtering

This variant of sputtering is used to deposit films of materials like oxides or nitrides by using pure metals as a targets. In addition to sputter gas like Argon, a reactive species (generally oxygen and nitrogen) were also introduced after the plasma ignition. The reaction between the target and reactive species takes in the plasma. A disadvantage is that the reactions happens at the sputtering target surface as well. target poisoning is seen considerable with higher flow rates of gases.

3. Magnetron Sputtering

It usually utilizes a strong electric and magnetic fields to trap electrons moving close to the surface of the target. The strong magnetic field lines bound the electrons to follow helical paths leads to more ionizing collisions with gaseous neutrals at the target surface than would otherwise left scattered. The higher the number of these collisions leads to a higher deposition rate. It also reflects that the plasma can be sustained at a lower pressure. And so the magnetron sputtering gives better quality films at low working pressure [26,27]. The $E \times B$ drift path shown in the figure, where the electrons are confined in a helical path by the magnets placed. behind the to increase the sputter yield

2.1.3.3 Components of Sputtering

The indigenously setup sputtering instrument requires components in order to monitor the conditions for of set parameters to deposit films.

1. **Chamber** : It is a stainless steel, round large volume enclosure where the complete mechanism happens. The diameter is of 44 cm and a height of 38cm roughly. The substrate holder is kept at the bottom and the target material is at the top with magnetron gun holding that. The distance between target to substrate is fixed at 5cm. A shutter is placed alongside the gun which is movable in both direction (clockwise and counter clockwise). Several holes are there to connect the gas inlet pipe, valves and gauges etc. The front glass window is for opening the chamber to insert sample into it.
2. **Magnetron Gun**: This assembly is at the top of the chamber consists of permanent magnets at the base in circular design. There are used for creation of magnetic field. Below this target is placed facing towards the chamber top part of the gun consists of inlet and outlet water connection for chiller with a point where negative electrode of power supply is connected.

3. **Gauges** : These are used for measuring lower order pressure inside the chamber.

Pirani Gauge: It is a thermal conductivity gauge which consists of metal filament suspended in a tube which is connected to the system. Due to flow of current the filament gets heated When this is suspended in a medium with lesser molecules will collide with wire and takes away the heat. The heat loss gives an indirect measurement of pressure. These gauges can read lower pressure in the range of 10^{-3} mbar order. It measures roughing and backing pressures in the system. [28].

Penning Gauge : It is also known as cold cathode gauge is used to measure vacuum. Application of high voltage between the anode and the cathode creates gas discharge and the resulting ionic current is measured with an ammeter. The measured amperes is calibrated into pressure units such as mbar , Pascals.[29]. These gauge is used for measuring higher order vacuum of about 10^{-3} to 10^{-6} mbar range.

4. **Pumps** : There are rotary and diffusion pumps for creating high vacuum in staged way.

Rotary Pump : This pumping is used for creating roughing stage vacuum inside the chamber, and then followed by in backing mode with the diffusion pump.

Diffusion Pump. It works in conjunction with rotary pump, it works on the principle of gas diffusion the heater heats up the silicone oil causes vapour to move upward through a vertical tapered hollow cone structure. This allows the oil vapour to escape at high speed which traps the air and then collide with water cooled surface and moves down. The trapped air is released at the bottom which is then sucked by rotary pump. It helps to attain the vacuum pressure up to 1×10^{-5} mbar Typical specifications of diffusion pump in the setup are :

Heater: 1250W, Oil Charge : 250cc (Silicone Oil) , Pumping Speed: 750 litres/sec .

5. **Mass Flow Controllers** : This device automatically controls the flow rate of a gas as per the set flow rate sent in form of electrical signal, without being affected by use conditions and changes in gas pressure.
6. **Gas inlet values** : This is the used to allow the gas or to isolate it to stop the gas inside the chamber.
7. **DC Supply** :A negative potential is applied a the top of magnetron gun through one end of this supply A maximum of1 KW power with variable voltage and current values can be set through knobs. Max Voltage is 1KV and current 1A.
8. **Chiller** : It is used to circulate cold water to the magnetron gun head as well as diffusion pump wall to extract heat from them. Its temperature is controlled automatically by temperature controller.
9. **Air intake** : Chamber is allowed to come under atmospheric conditions through this value. This is done by rotating in anti-clockwise direction.



Fig 2-7: DC Magnetron Sputtering for TiN thin film Deposition

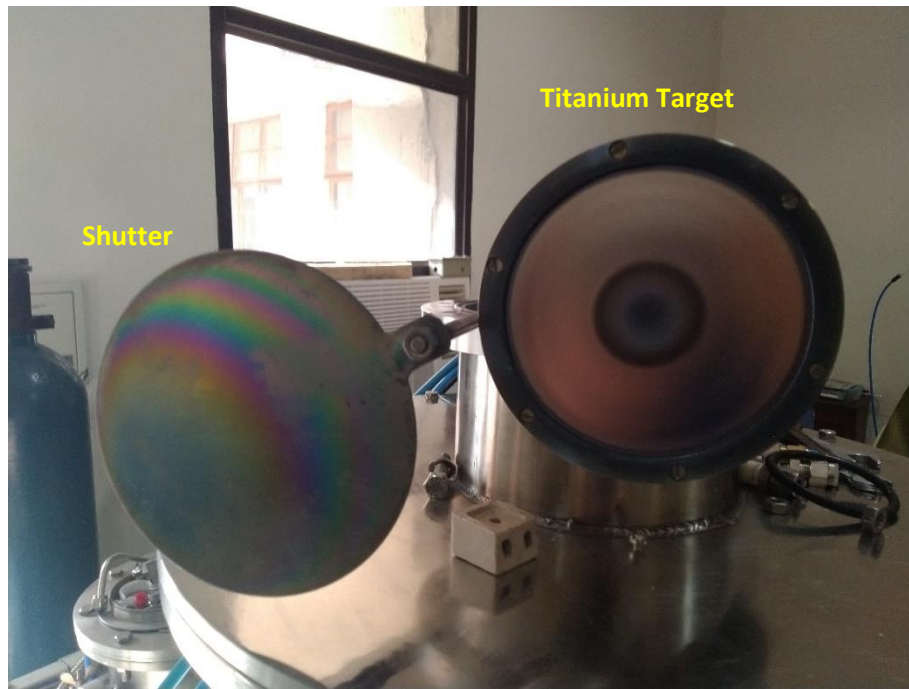


Fig 2-8 : Shutter and Target in a Magnetron Gun Assembly

2.1.3.4 Sputtering Parameters

The Performance of any sputtering depends on various factors like geometry of Target and substance distance, (Diameter of Substrate holder and Target), distance between target to substance, rate of deposition which is depended on target power and Working Pressure. The evaluation of system performance with respect to these factors are crucial. In this section, there is brief discussion on the influence of process parameters on the properties and composition of Titanium.

Deposition Parameters Evaluation

Titanium Thin Film were deposited using DC reactive sputtering. A study of process parameter for deposition of films are :-

1. Rate of Deposition for different target Power

With increase in target power for a given pressure and other parameters same, will lead to an increase of the plasma density and hence higher Ar^+ ion density at the target surface. This causes more number of target (Titanium) atoms to sputtered out. This leads to an increase in film deposition rate.

2. Working Pressure

The relationship between sputtering pressure and mean free path (λ) is governed by [30]

$$\lambda = 2.330 \times 10^{-20} T / P \delta_m^2 \quad (2.2)$$

T(K) is temperature, P (mbar) is working pressure and δ_m^2 (cm) is the molecular diameter. From the

equation, it is clear that the working pressure is inversely proportional to the mean free path. If the mean free path is low; the sputtered atoms experience large number of collisions with the background gas which results in scattering. Hence, lesser number of atoms will be reaching the substrate. Whereas at lower pressure, the mean free path will be high, so scattering collision decreased and number of atoms reaching the substrate will be high.

3. Deposition Time

Time has profound effect on thickness of the film. It is a proportional relationship which can be physical understood that if the sputtering process occurs for larger interval of time, more and more target atoms will get deposited that results in increment in thickness of films.

4. Target to Substrate distance(TSD)

When an energetic ions passes through the plasma, it get scattered and losses energy by collisions and move in random direction. It can be visualizing like this that if the TSD increases, the probability of collision can be increased. Hence lesser number atoms reach the target that results in lower thickness values.

2.1.4 Preparation of Sample

A100mm diameter of n-type silicon substrate (polished) were taken from a lot which is cut down into 4 quarters with the help of diamond cutter. Before using for depositing the first step is of cleaning the samples. Microscopic glass slides were used in the deposition

2.1.4.1 Cleaning:

This step is the first step for fabrication towards MIS device. It is done to remove the native Silicon dioxide layer along with the other impurities existed in the sample. For this the cut down silicon were kept in the jig. The cleaning procedure is done in three steps Firstly, the jig containing the Silicon was fully immersed in a beaker filled with acetone followed by ultra sonication for 5 minutes. It removes the organic contamination. Before going for different chemical treatment, an intermediate deionized(DI) water rinsing for a 1 minutes is performed. Secondly, HF solution (2-4 %) with water was used for next step cleaning. It makes the surface hydrophobic. This step is performed for 2 minutes It helps to remove thin layer of the native oxide. Pirana Solution is a mixture of Sulphuric acid to hydrogen peroxide in 4 :1 ratio. As per the ratio definite amount was chosen so that complete sample can be immersed in water. The solution temperature should be around 80°C and were immersed inside for 10 minutes, the samples were rinsed with DI with water and then final HF treatment for a duration of 2 minutes

The Glass samples were cleaned by ultrasonication with acetone to remove fingerprint marks or any other impurities.

Finally drying up with air blower to remove the remaining water droplet stick to the surface. The drying of cleaned wet substrates is also critical to reduce probable recontamination due to adsorption of gaseous particles and dust.

2.1.4.2 Sputtering Process for TiN thin films

A Pure Titanium target was loaded at the bottom of the magnetron gun which serves as the target material. A small strip of n-type polished silicon is loaded with glass (50mm x 25mm x 1.3mm) is placed at the centre of substrate holder. The deposition chamber was evacuated through rotary pump at roughing initially then followed by Diffusion Pump backed by rotary pump. The chiller was used to circulate cold water to magnetron gun and the side walls of the diffusion pump. A roughing pressure was attained by using roughing pump of the order 4×10^{-2} mbar The bidirectional valve is turned downward in backing mode for the diffusion pump. When the backing pressure is reached, the Diffusion pump is turned on , and allowed to get heated for 30 minutes. Then the baffle valve was opened which connects the diffusion pump to the chamber. The chamber pressure is brought to vacuum level of 2×10^{-5} mbar which acts as base pressure. A high quality of Argon (99.999% pure) and Nitrogen (99.9999% pure) was used as sputter and reactive gas respectively. Gases were flown through Mass Flow Controller to set precise flow into the chamber. Initially Argon gas was used for creating plasma at a specific conditions of power (340 V, 0.24 mA) through a DC power supply, working Pressure of 5×10^{-3} mbar was maintained by controlling the opening of the baffle valve. Rate of argon flow is maintained at 5 SCCM through a mass flow controller to ignite the plasma, then followed by Nitrogen gas desired rate for a particular sample for a set duration. To remove oxide layer on the target, the target has been pre sputtered for 10 min. After that deposition on substrate is started by removing the shutter. During the process, the conditions were monitored for any changes

Deposition Parameters

Table 2-2 : Parameters used for film deposition in DC Magnetron sputtering

| | |
|---------------------------|---|
| Power Source | DC Power Supply (1KV 500mA) Range |
| Sputtering Target | Pure Titanium (100mm diameter and thick) |
| Substrates | Glass(50mm x 25mm x 1.3mm) , Silicon(n type) |
| Base Pressure | 2.3×10^{-5} (mbar) |
| Working Pressure | 5×10^{-3} (mbar) |
| Target Power | 80Watts |
| Target to Substrate dist. | 5 cm |
| Deposition Time | 30 min , (10 , 20 , 40 mins for time variation set) |
| Nitrogen Flow | 2.5 , 5 , 7.5 , 10, 12.5 , 15 , 20 , 25 (SCCM) |

| | |
|------------|---------------|
| Argon Flow | 5 SCCM(fixed) |
|------------|---------------|

2.1.4.3 Annealing of TiN deposited Silicon Samples

For MIS device preparation, a piece of sample was cut into define size and kept in the slots of substrate holder inside quartz tube. The samples were heated at 450°C in a temperature controlled Muffle Furnace. For a period of 30 minutes. Before starting the procedure, nitrogen was purged inside the tube to remove contamination for 5 minutes. Hydrogen flow supply was kept at 60 psi, once it reached the outlet valve is opened which is connected to the inlet of tube. The hydrogen was maintained throughout the duration of annealing of samples. All samples that were prepared through sputtering at various conditions, annealed at one go. After the completion of 30 minutes, hydrogen flow was still maintained for another 20 minutes so as to slowly reach to room temperature. After that samples were ready for final step of metallization.

2.1.4.4 Metallization

The final step for MIS device was the contact making through Electron-Beam Evaporation. The deposition took place at a base pressure of 3×10^{-6} mbar was used for both front and back. Aluminium coating for contact is created at the front and back of uniform thickness of 500nm. The front contact is small dot (0.0078 cm^2 area) structure whereas the back is fully coated.

2.2 Characterization Techniques

In order to see the different properties associated with Titanium Nitride thin film, we need several measurements that are performed by different instruments. The knowledge of the working of these instruments is necessary to extract the outputs from it.

2.2.1 UV-Vis-NIR Spectroscopy

Light incident on any material undergo three basic phenomena that is transmission, absorption and reflection. To study the light interaction with the thin film we need to create the conditions of the spectrum and understand how the film responds to it. Let us consider the film has refractive index, n , coated onto a substrate of refractive index s , then there are three interactions at the air-film, the film-substrate and substrate-air interfaces, part of the incident intensity is reflected and part is it is transmitted. From fundamental considerations of optics it follows that since the reflected and transmitted beams originates from a single coherent source, the beams will exhibits interference. The objective here is to see maximum level of transparency for our Titanium nitride thin films, UV-Vis spectroscopy is needed to measure the transmittance values over the entire wavelength range starting from Near Infrared to Ultraviolet.

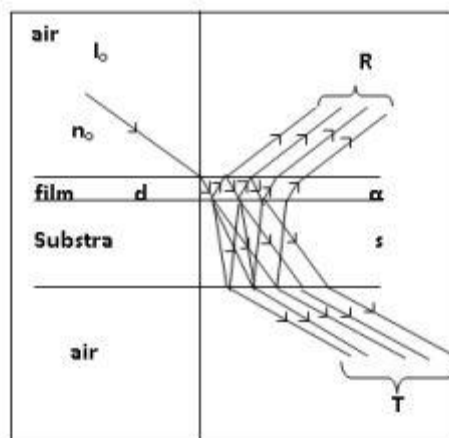


Fig 2-9: Interference from a thin film deposited on thick substrate, $s \gg d$.

The spectrophotometer consists of two types of lamps one is Hydrogen Deuterium Lamp and the other is the Tungsten Halogen Lamp. The former is for producing UV light and the later is for the rest of spectrum (Visible and Near Infrared Regions). This spectrophotometer has the ability to swap lamps when it is producing light from NIR to UV region. The light from the lamps are directed towards the single or double monochromators. The monochromator is a combination of of entrance slit, lens gratings or prism and an exit slit. The light is first passed through the entrance slits and then followed by the collimating lens which focus the lights towards the gratings. The focused light is dispersed by the holographic grating into seven

parts called VIBGYOR in the monochromator or commonly called spectrograph. The optimum light is then taken out from exit slit. After that a rotating chopper splits the light which is then guided by the mirrors, one for the sample and other for reference. One part of the light strikes the sample and the other part strikes the reference. The light passing through both are analyzed by the different kind of detectors.[31] The detectors present at the end of sample and reference to detect the light and converts to equivalent to electrical signal. The commonly used detectors in UV-Vis Spectroscopy are :-

- Photo multiplier tube (PMT) detector: In this the photons striking the PMT detector gets converted into electrons and are also multiplied.
- Photodiode array (PDA) detector: Diodes are utilized which converts electromagnetic radiation or UV-Vis radiation into electrical signals.
- Charged coupled Detector (CCD): In this there is a silicon surface and when radiation in the form of photon strikes this silicon surface and will be converted into digital signals by using CCD

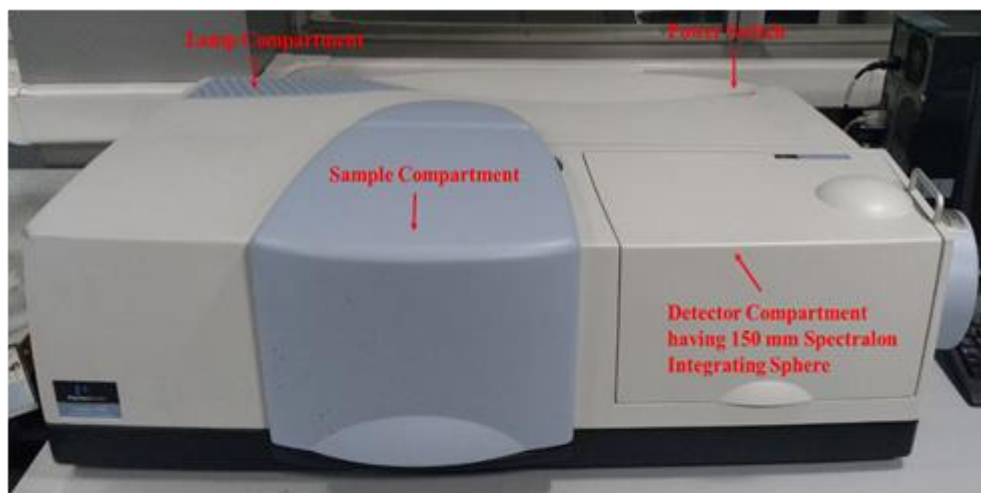


Fig 2-10: UV-ViS-NIR Spectrophotometer, (Make : Perkin Elmer Lambda 1050)

The detected signal is then transferred to computer through a data acquisition system and a required software for interfacing and giving commands to the instrument.

The instrument used here is Perkin Elmer Lambda 1050 which is a high performing spectrophotometer designed for analysis of coatings, glass, and components in both research and manufacturing. It covers wavelength range covering from 175nm to 3300nm. This range covers Ultraviolet, Visible and Near Infrared Lights.

The lambda 1050 instrument consist of three detector module attachment which contains three detectors PMT, InGaAs and PbS. which are responsible for catching light at different wavelength.

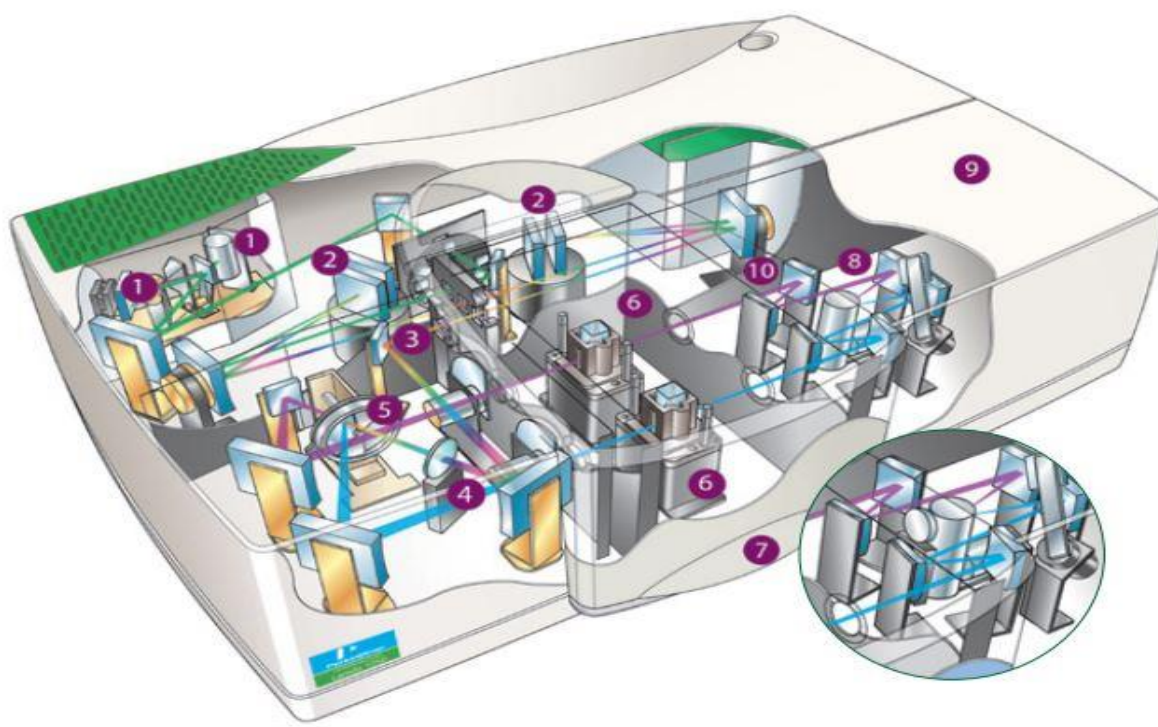


Fig 2-11 : Inside the spectrophotometer

Components of UV-Vis Spectroscopy [32].

1. Deuterium and Tungsten Halogen Light Sources that are Pre aligned and pre focused , it utilizes a source doubling mirror for better sensitivity.
2. Double Holographic Grating Monochromators for ultra-low stray light performance.
3. Common Beam Mask that allows precise adjustment of beam height to match samples of different dimensions.
4. Common Beam Depolarizer which Corrects for inherent instrument polarization to allow accurate measurements of birefringent samples (optional).
5. Chopper Switches between sample and reference beam. Four-segment design provides individual blank readings for sample and reference
6. Sampler and Reference Beam Attenuators that are used for accurate measurements and extremely sensitive on highly absorbing samples.
7. Largest Sample Compartment to allow easy access to a wide variety of sampling accessories and sample types.
8. High-sensitivity Photomultiplier and Peltier-controlled PbS Detectors that provides full range UV/Vis/NIR coverage from 175 to 3300 nm (LAMBDA 950).
9. Second Sampling Area : houses a range of snap-in sampling modules including transmission optics 150 mm integrating spheres and universal reflectance accessory
10. High-sensitivity Photomultiplier, Peltier-controlled InGaAs and PbS Detectors.

2.2.2 Electrostat/Potentiostat

This instrument is required for the electrical characterization of MIS Device, basic measurement of capacitance voltage (C-V) , Electrochemical impedance spectroscopy (EIS) and current voltage(I-V) are performed for titanium nitride thin film MIS device structure using Gamry Instruments Reference 600 Model.

It is an electronic instrument that basically controls the voltage difference between a Working Electrode and a Reference Electrode. Conventionally, it found its application in electrochemistry, where both electrodes are contained in an electrochemical cell. The potentiostat implements this control by injecting current into the cell through an Auxiliary, or Counter, electrode. In almost for all applications, the potentiostat measures the current flow between the Working and Counter electrodes. The controlled variable in a potentiostat is the cell potential and the measured variable is the cell current. In general there are five important electrodes that are used in the Electrostat/Galvanostat for measurement These are combined together in a specific configuration to measure the parameters. The systems are classically developed for the purpose of electrochemistry but its application are in wide areas.[33]

Working Electrode

The electrodes is used for measuring current by controlling the potential. Common used working electrodes are made of inert materials such as Au, Ag, Pt, glassy carbon (GC) and Hg drop and film electrodes etc.

Reference Electrode

The reference electrode is an electrode which has a stable and well-known electrode potential and it is used as a point of reference in the electrochemical cell for the potential control and measurement. The Reference Electrode is used to measure the Working Electrode potential. A Reference Electrode should have a constant electrochemical potential as long as no current flows through it.

Counter (Auxiliary) Electrode

The Counter, or Auxiliary, Electrode is a conductor that completes the cell circuit.



Fig 2-12: Electrostat/Potentiostat Gamry Instruments Reference 600 Model

2.2.2.1 Electrochemical Impedance Spectroscopy

Conventionally, Electrochemical impedance spectroscopy (EIS) is powerful and mostly used technique for the characterization of electrochemical reaction and properties of materials. EIS measures the impedance of the electrochemical system over a wide range of frequencies. In general, any real world physical device can be considered as elements of an equivalent electrical circuit that include combination of capacitor, inductor and resistor.

Impedance is the measure of the ability by which it resist the flow of electrical current in the circuit. And it is affected by the frequency unlike the ideal case of resistor which is independent. If an small ac sinusoidal signal is applied to the system, the response is produced is sinusoidal with the same frequency but only shifted in phase. From this we can infer that impedance of system consist of two main information i.e change in amplitude between the applied and measured signal and the phase shift that reveals the resistive and reactive nature of the system.

Assume that we apply a sinusoidal potential excitation. The response to this potential is an AC current signal. A complex plot is required for the representation of the impedance value, because it can carry all the information of real, resistive and imaginary, the reactive part. Electrochemical Impedance of the sample

is measured by using small signal excitation superimposed over the DC bias. The plot between the real and the imaginary is known as Nyquist Plot.

In the study the application of EIS is to look for the variation of real axis impedance and the imaginary axis impedance as sweep the frequency. The main interesting feature of EIS is that it provides information at each frequency. This data is utilized in deriving various values for the device.

2.2.3 Quantum Efficiency(QE) and Current Density(J_{sc}) – Voltage(V) Measurement

Quantum Efficiency(QE) is an important device parameter related to performance of the solar cell. The standard test conditions being 100 mW/cm² AM 1.5G at 25°C. Mathematically QE is defined as the ratio of number of carriers collected by solar cell to that of number of photons of given energy is incident on the solar cell. It provides information about recombination process active in the material and also about the quality of the passivation layer. The QE measurement provides qualitative information whereas the J-V characteristic provides estimation of the maximum power that can be extracted from the solar cells.

There are two types of Quantum Efficiency one is Internal(IQE) and the other is External(EQE). EQE is defined as the ratio of the number of electrons that are collected by the solar cells to the number of photons of a given energy incident from outside. IQE is defined as the ratio of number of the electrons that are collected by the solar cell to the number of photons of a given energy absorbed by the solar cell.[34].

$$IQE = \frac{EQE}{1-R(\lambda)-T(\lambda)} \quad (2.2)$$

$$EQE = \frac{\Delta J_{sc}}{q\Delta\phi_{\lambda}} \quad (2.3)$$

The ΔJ_{sc} represents the increment in short circuit current generated by the solar cells for incident incremental photon flux of $\Delta\phi_{\lambda}$ at a wavelength of λ . The main difference between EQE and IQE is that EQE does not include the transmission and the reflection losses while the IQE include both the optical losses.

In order to measure QE and J-V characteristics of samples M/s Bunkoukeiki (Model: CEP-25HS 50) is used which can hold samples having maximum size of 5cm x5cm. Limitation in the size because of illumination source uniformity. In this set-up light source is Xenon lamp and its light is guided through suitable optics to the sample stage.

For the J-V measurement, an AM 1.5G filter is used for white source (100mW/cm²). On the other hand in order to measure the QE, there are grating monochromator based optical filters and a set of optical assembly, lock in amplifier, etc. and the wavelength can be varied by steps of 1 nm to 50 nm. In this spectral response

(SR) measurement, the photocurrent density from the solar cell is measured with respect to monochromatic light of specific wavelength of. fixed intensity. The SR is measured in the spectral region 300-1200 nm. EQE can be determined using the following relation,

$$SR = \frac{q\lambda QE}{hc} \quad (2.4)$$

Where q is referred to as the electronic charge, λ is the wavelength of the incident light, h is the Planck's constant and c is the velocity of the light.

This J-V measurement under the standard test condition of illuminated radiation is the primary characterization test of a solar cell device. From this characterization curve obtained we can calculate all other cell parameters and also the power conversion efficiency of the device. The Xenon lamp being the source of radiation, its intensity and operation is controlled by the power supply system. As mentioned earlier the light from the xenon lamp is passed through an AM 1.5G filter which says that the light is AM 1.5 G is of stipulated intensity. Before any measurement, the intensity of the Xenon lamp is measured using a standard photodiode which is used as a reference cell.



Fig 2-14 : I-V and SR measurement system, M/s Bunkoukeiki (Model: CEP-25HS 50)

CHAPTER-3

Results and Discussion

3.1 Optical Measurement

The optical measurement includes Transmission characteristics of the prepared thin film on glass slides. The interval chosen is from 2400 nm to 300 nm at a step of 2nm.

3.1.1 Transmission with nitrogen Flow Rate

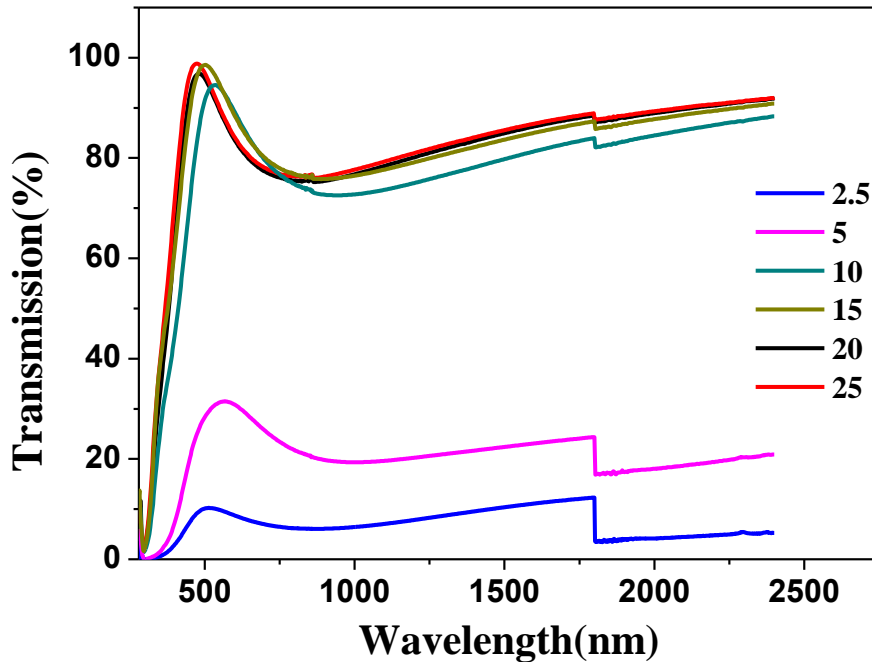


Fig 3-1: Transmission (%) for different nitrogen flow rates

The fig:3-1, shows the change in Transmission with varying nitrogen flow rate, it reveals that from lower nitrogen flow the transmission(%T) of films is on the lower side, for low flow rates up to 5SCCM, the transmission of films is low compared to other rates. Drastic increment on the property can be seen for flow rates > 5 SCCM. There after there is not much significant rise on transmission of films from 10 SCCM. But there is slight increment in %T is observed in IR range and corresponding a slight dip in the Visible region as it starts to rise from 1000 nm for flow greater than 10 SCCM. Also the peak of the curve shifts towards the UV region, with flow rate increments after 10SCCM. Keeping in mind the %T values in visible region is found better for flow rate of 15 SCCM.

3.1.2 Transmission with Deposition time variation

The fig:3-2, shows that the variations of Transmission with variation in deposition of time, The distinct curves clear indicates change in transmission of films. For shorter deposition time, the transmission of films is higher than that of for longer deposition time. For 30 min, it shows better %T.

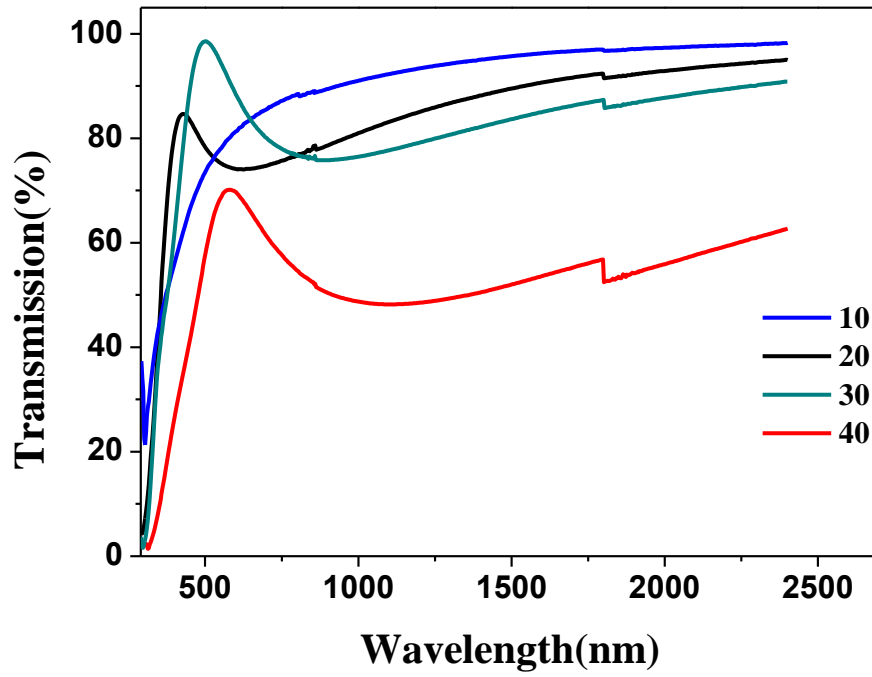


Fig :3-2 : Transmission (%) for different deposition time

3.2 C-V curves of the samples

3.2.1 Influence of Nitrogen flow Rate

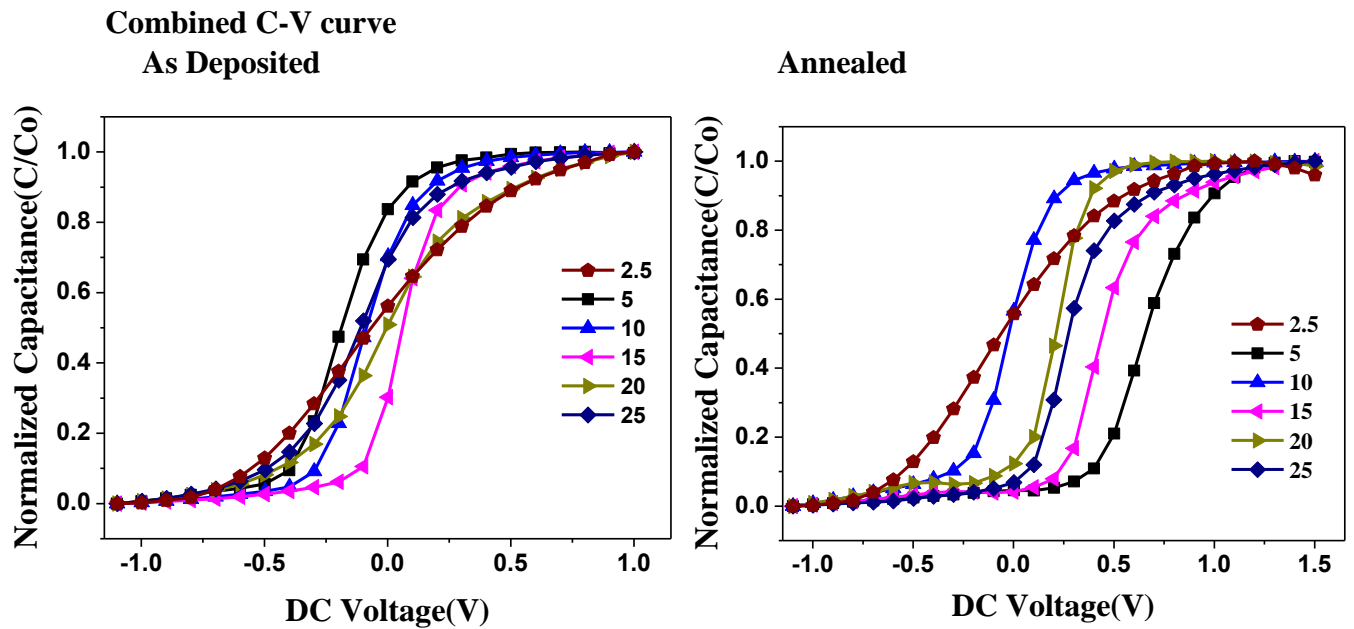


Fig 3-3 : Combined C-V curve at 1Mhz of (a) as deposited and (b) annealed with flow rate

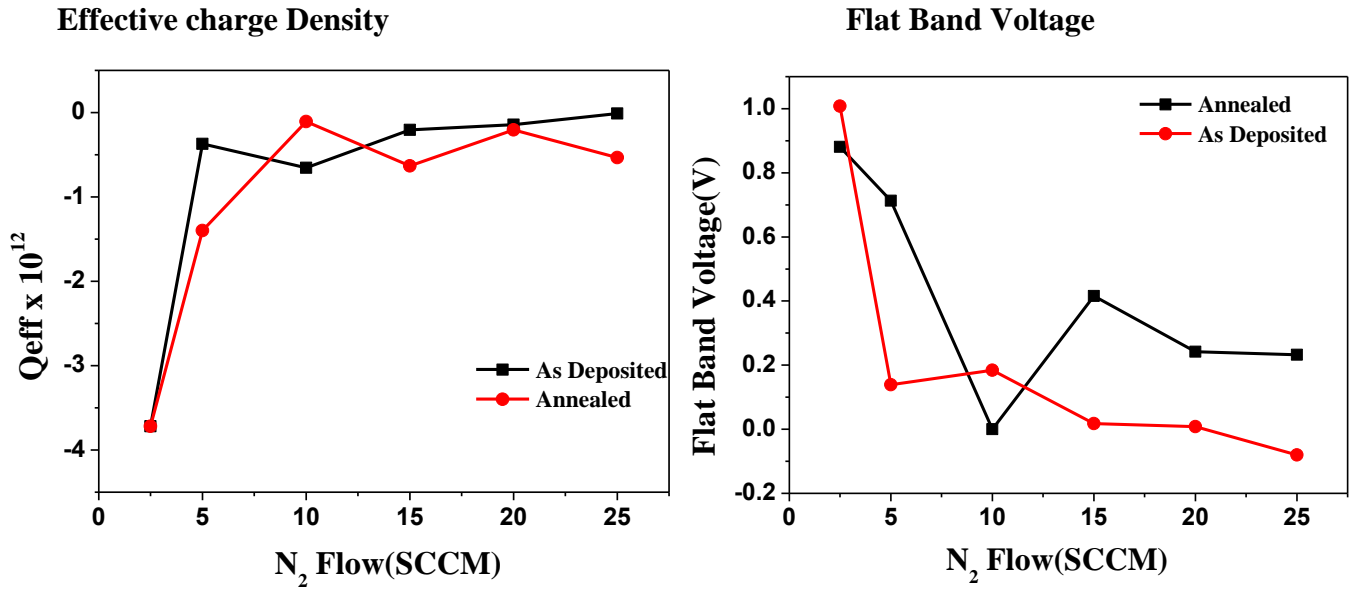


Fig 3-4: (a)Effective charge density vs flow rate for as deposited and annealed
(b)Flat Band voltage vs Nitrogen Flow for as deposited and annealed

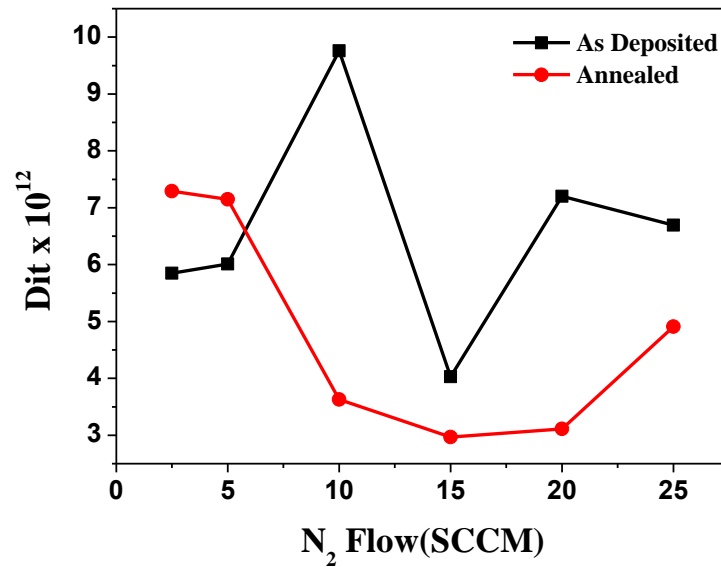


Fig 3-5:Dit values for various Nitrogen Flow

Table 3-1 : Q_{eff} , V_{fb} and Dit values for as deposited and annealing samples for different flow rates.

| Sl No | N2 Flow (SCCM) | As deposited Q_{eff} ($C.cm^{-2}$) | As deposited V_{fb} (Volts) | As deposited Dit ($cm^{-2}eV^{-1}$) | Annealed at 400C Q_{eff} ($C.cm^{-2}$) | Annealed at 400C V_{fb} (Volts) | Annealed at 400C Dit ($cm^{-2}eV^{-1}$) |
|-------|----------------|--|-------------------------------|---|--|-----------------------------------|---|
| 1. | 2.5 | -3.72×10^{12} | 1.008 | 5.84×10^{12} | -3.72×10^{12} | 0.881 | 7.29×10^{12} |

| | | | | | | | |
|----|----|------------------------|-------|-----------------------|------------------------|-------|-----------------------|
| 2. | 5 | -3.71×10^{11} | 0.139 | 6.01×10^{12} | -1.40×10^{12} | 0.713 | 7.14×10^{12} |
| 3. | 10 | -6.55×10^{11} | 0.184 | 9.75×10^{12} | -1.07×10^{11} | 0.03 | 3.62×10^{12} |
| 4. | 15 | -2.06×10^{11} | 0.018 | 4.02×10^{12} | -6.31×10^{11} | 0.416 | 2.96×10^{12} |
| 5. | 20 | -1.43×10^{11} | 0.008 | 7.20×10^{12} | -2.05×10^{11} | 0.242 | 3.10×10^{12} |
| 6. | 25 | -1.10×10^{10} | -0.08 | 6.69×10^{12} | -5.34×10^{11} | 0.232 | 4.90×10^{12} |

In this study n-type Silicon Substrate is used, the fig : 3-3(a) ,shows the curve of as deposited samples measured at frequency 1 MHz. The curve behaviour varies with different flow rate which is supported by the change in flat band voltage of the as deposited voltage from fig 3-4(b). all the flat band voltage for all the samples lies in the positive bias range. This confirms the presence of negative fixed charge carriers in the as deposited one.

After annealing, for samples having flow greater than 15(SCCM) there is reduction in effective charge density which is supported by a positive shift in the flat band voltage. For all the samples there is moderate level of effective charge density. However there is substantial decrease in the D_{it} values in the order of $10^{11} \text{ cm}^2\text{eV}^{-1}$. From table 3-1, the D_{it} value of flow rate 15 and 20 are least among the other annealed one. And the effect of annealing is prominent in flow rate of 10 and 20 SCCM. For the flow rate of 15 SCCM, from fig3-5, shows the variation of D_{it} values with the flow rate,the D_{it} value of as deposited samples have values lower than that of annealed D_{it} values of samples prepared at other flow rate. Lower D_{it} values shoes better chemical passivation property and hence nitrogen flow at 15 is the optimum condition. And annealing of the sample reduces a bit hence annealed sample of flow 15(SCCM) is the optimized condition

3.2.1.2 Influence of hydrogen annealing on flat-band voltage:

In order to understand the variation of defects/fixed charges at the interface, the devices were subjected to annealing under H_2 ambience and the capacitance was recorded at 1MHz.it was commonly observed that the C-V curve shifted positively after hydrogen annealing, indicating that H_2 annealing induced negative fixed charges in the dielectric film. However, for the films deposited at $\text{N}_2=10$ SCCM, the shift is nominal, representing the lower interface defect density as seen from the variation of defect density with respect to N_2 flow. As a result hydrogen might not have form allotropic forms of H^{3+} .

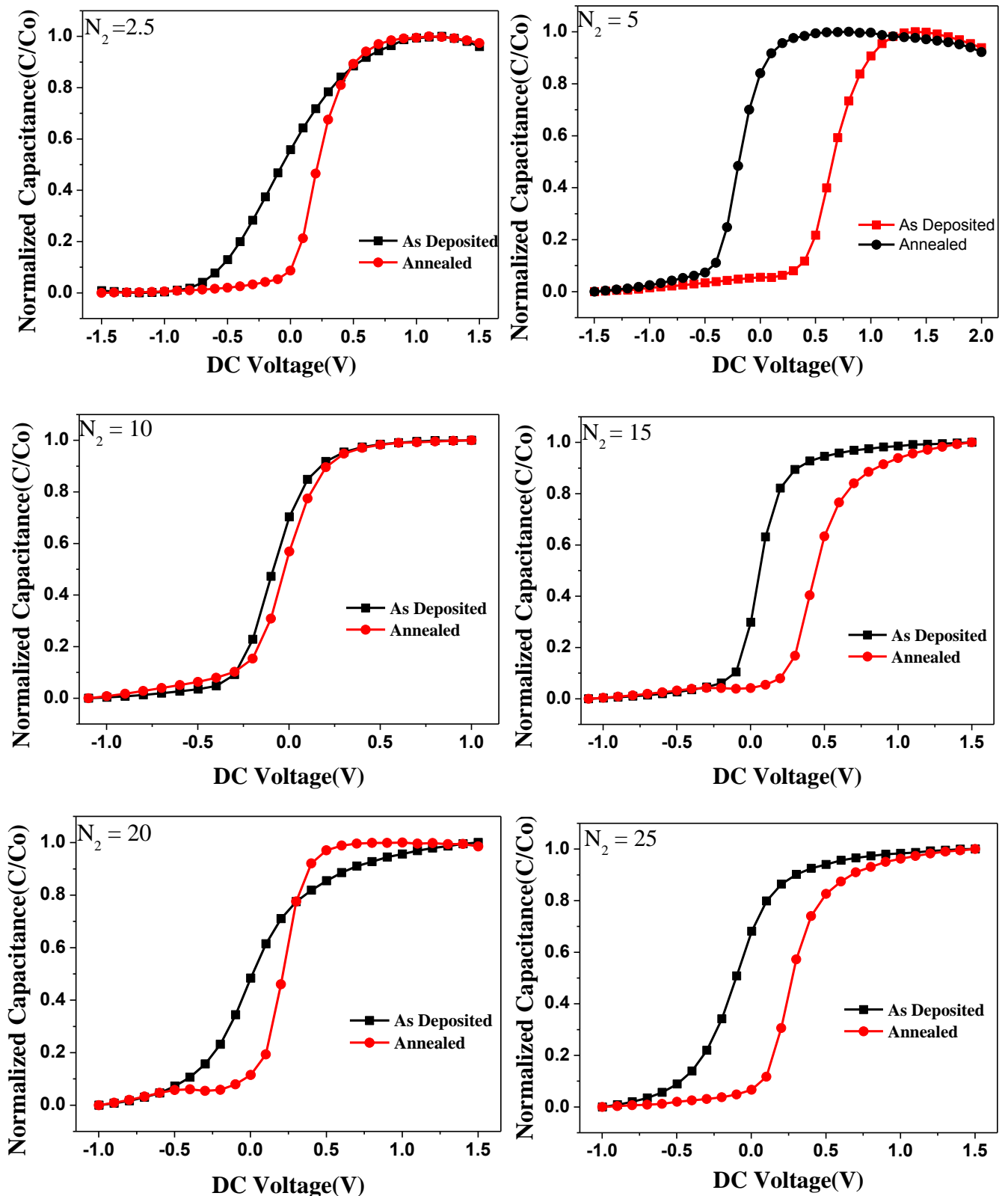


Fig :3-6 : C-V Comparison between as deposited and annealed at 1Mhz .

3.2.1.3 Nature of the traps

Frequency dispersion the C-V spectrum of the devices for different N_2 flow rates shows the nature of defects changes with respect to the flow rate. It can be observed from the figures that the sample deposited for the flow rate of 15 SCCM has less defect density.

As Deposited

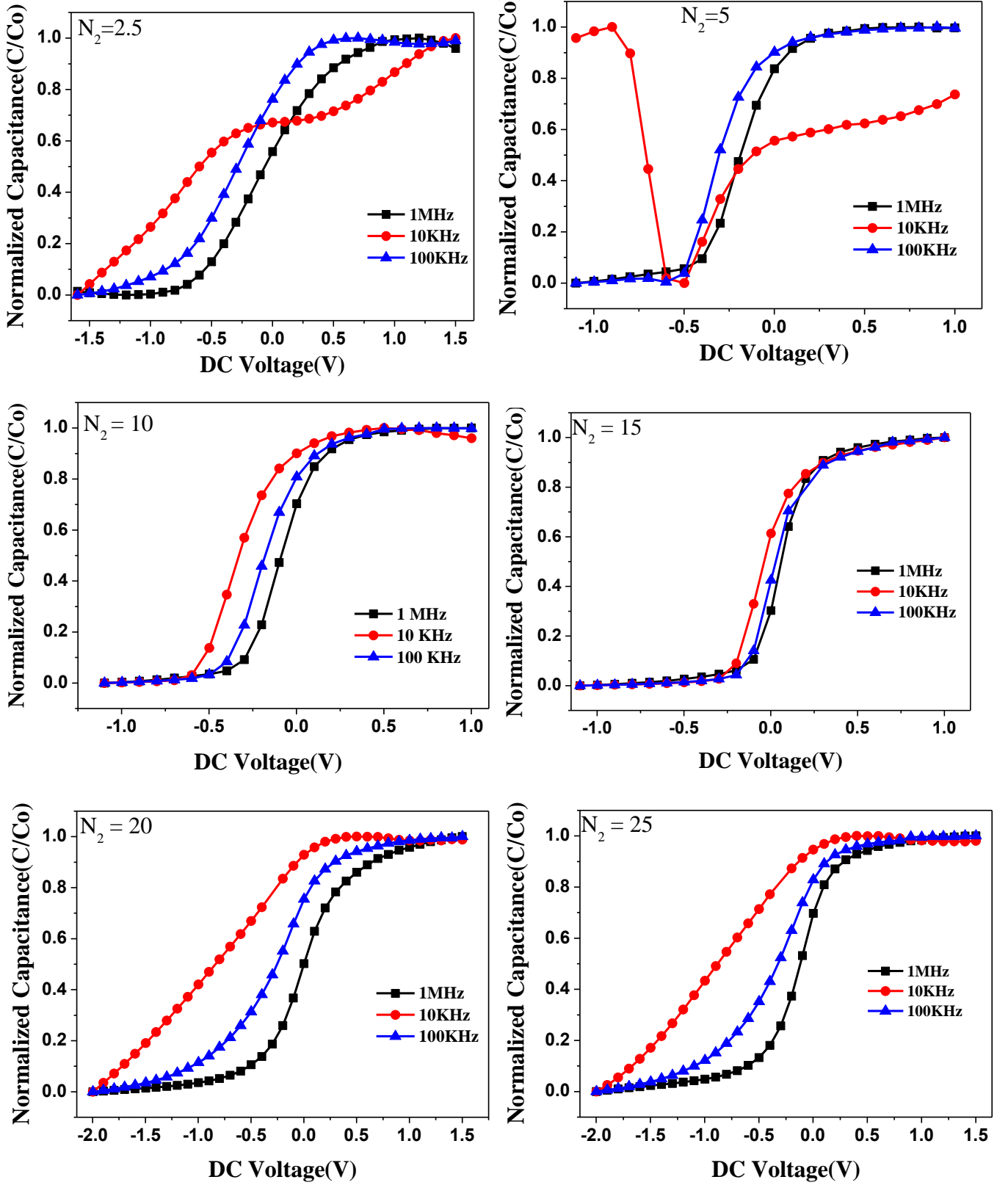


Fig:3-7 : Trends in C-V curve of as deposited for different frequency with flow rate variation

Annealed Samples

As per the results shown in the figures, the frequency dispersion of the C-V curves is less in comparison with as-deposited films, inferring that hydrogen passivated the interface defects.

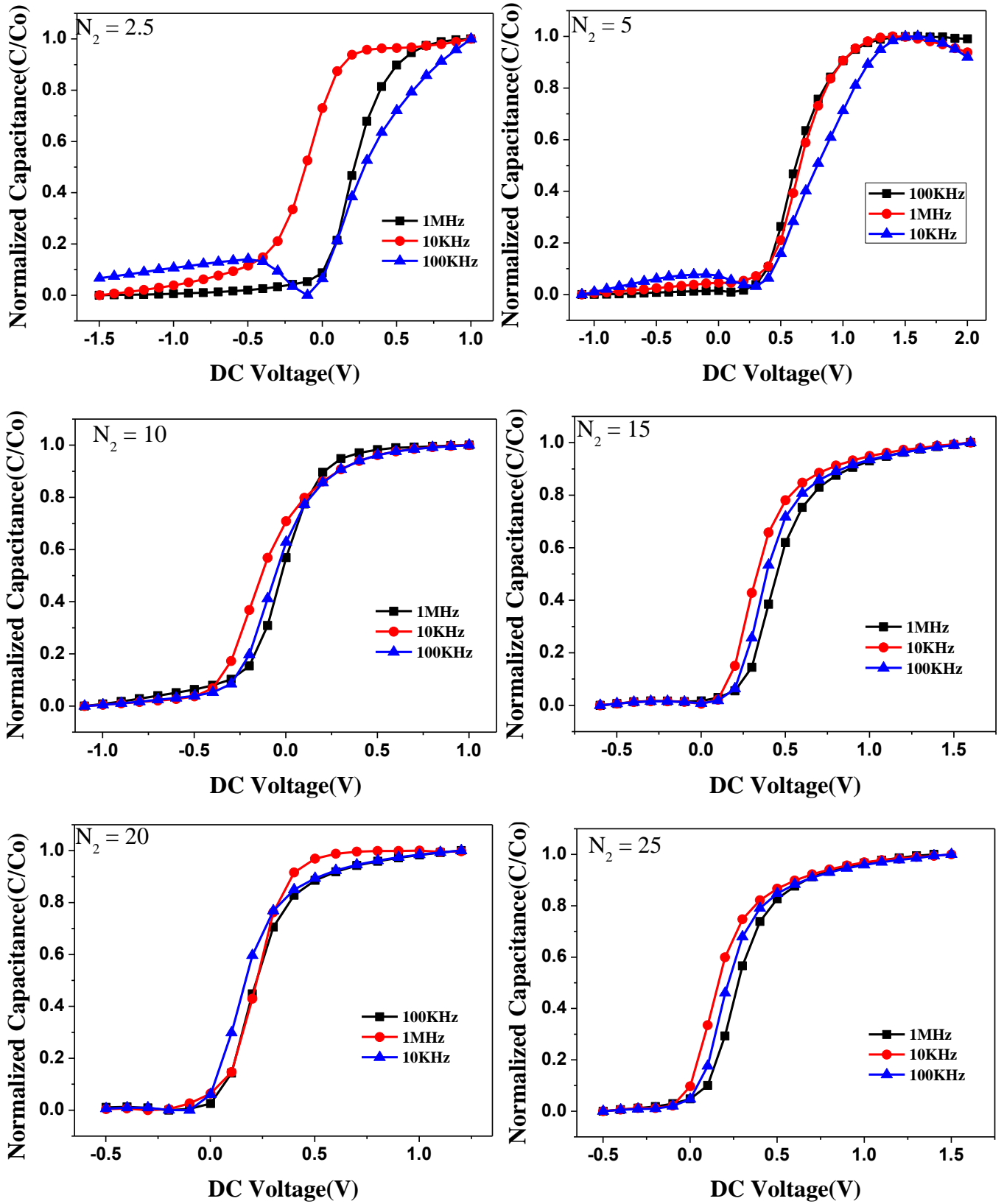
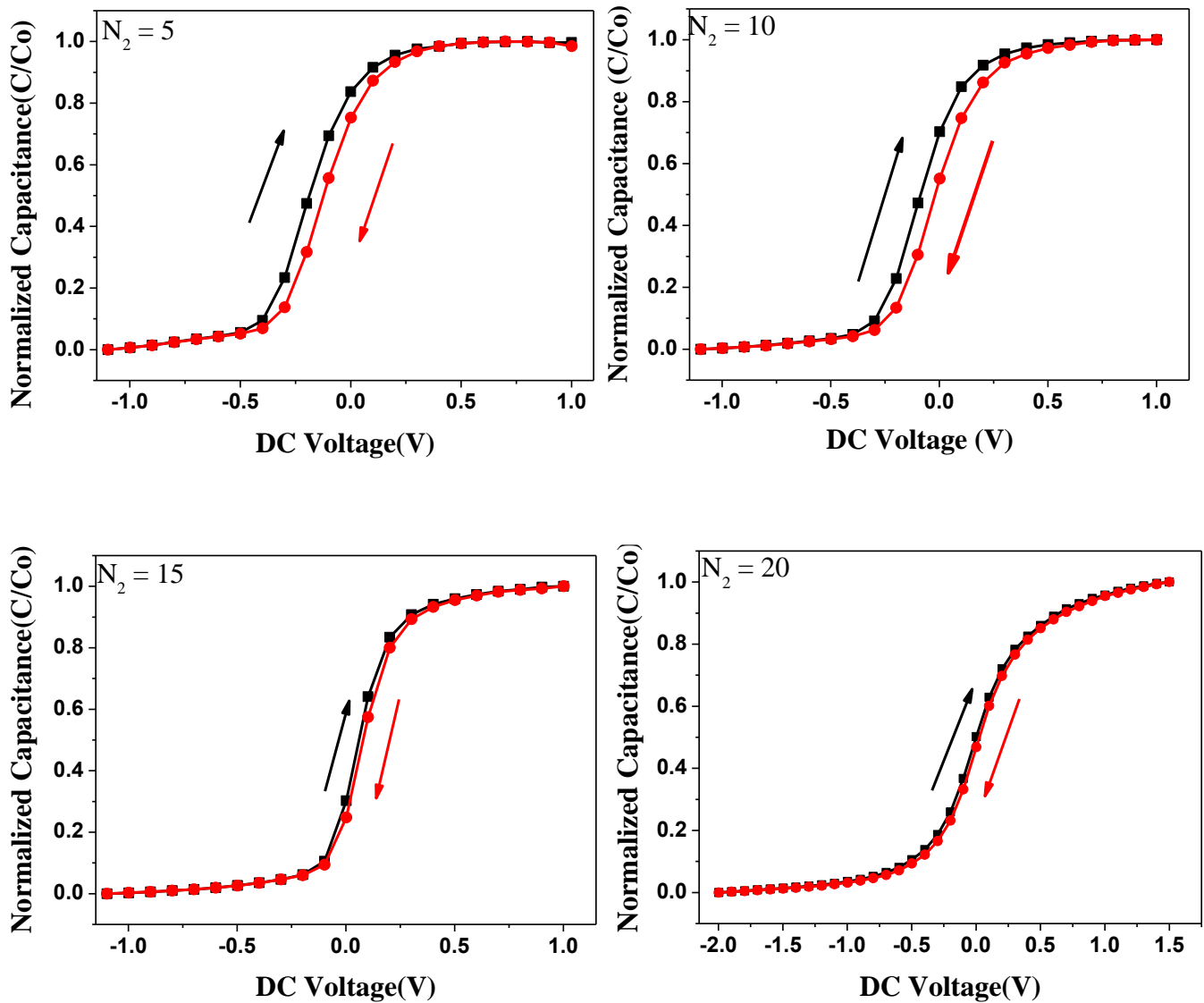


Fig :3-8 : C-V curve with different frequency variation for annealed samples with flow rate

3.2.1.4 Effect of traps at the interface

As Deposited

The presence and nature of interface defects influence that trapping and de-trapping mechanism at the interface, which can be understood from the capacitance behaviour of the device when swept in both the directions. For the films deposited above the N₂ flow of 10 SCCM, the traps are categorised as fast-traps in nature. influence of sweep direction affects the behaviour of the C-V curve due to presence of traps. Mobile charges are affected by it the most.



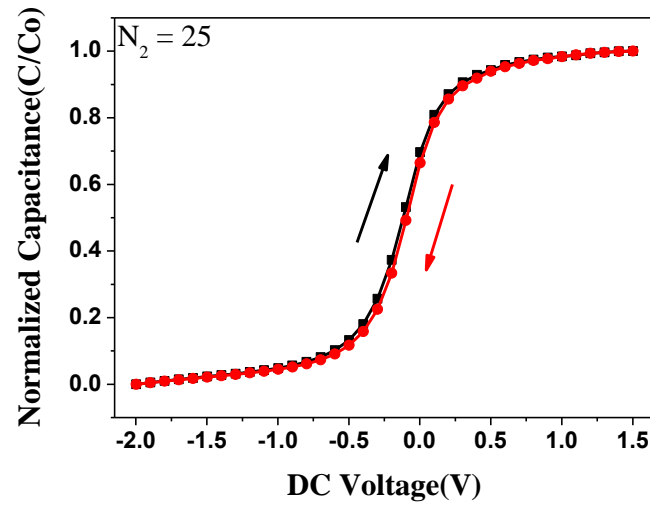
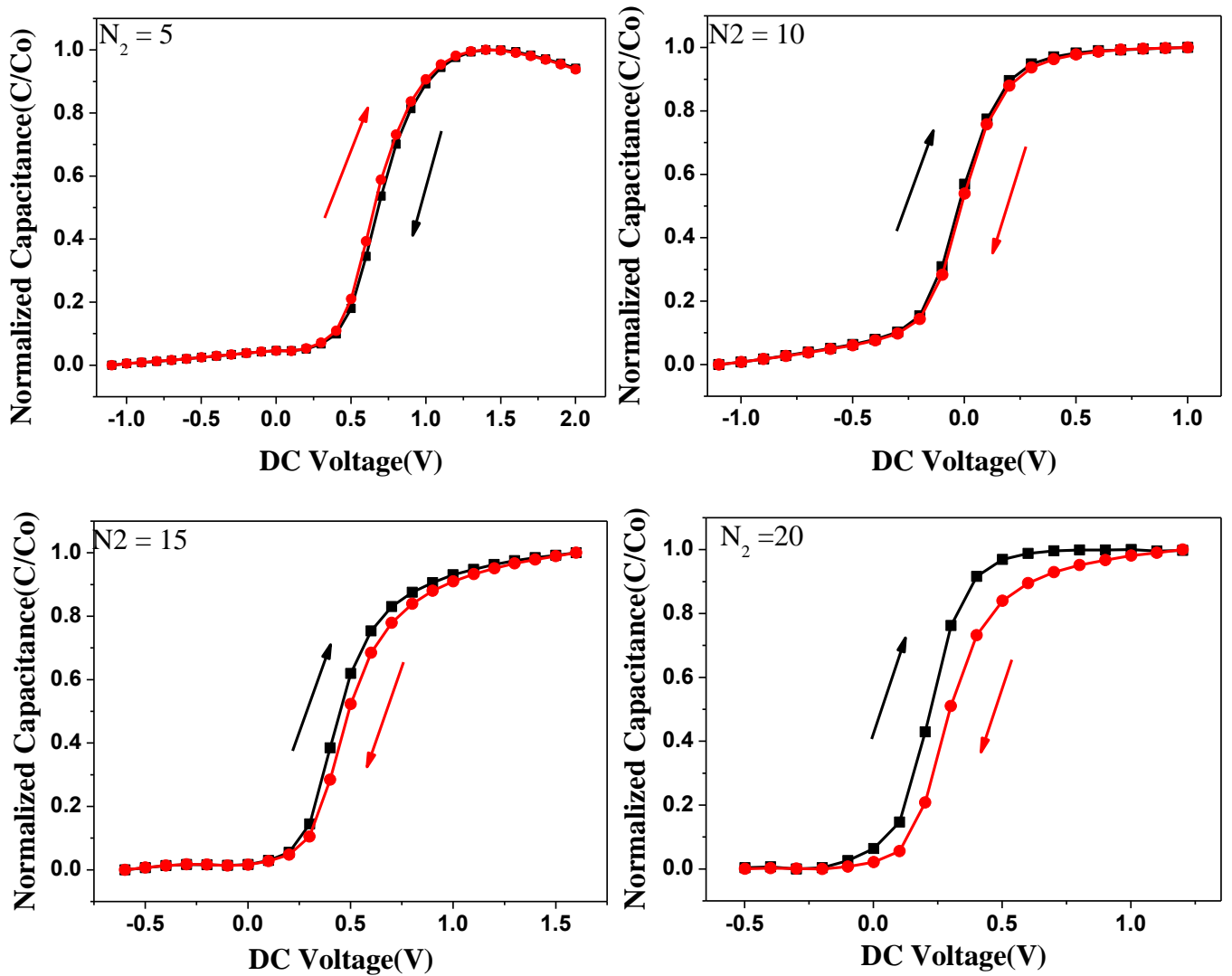


Fig 3-9 : Effect of sweep direction for as deposited samples with flow rate

Annealed

After the hydrogen annealing, the interface defects are healed. For the films deposited at the flowrates, $> 10\text{SCCM}$, the annealing created the additional defects/charges at the interface.



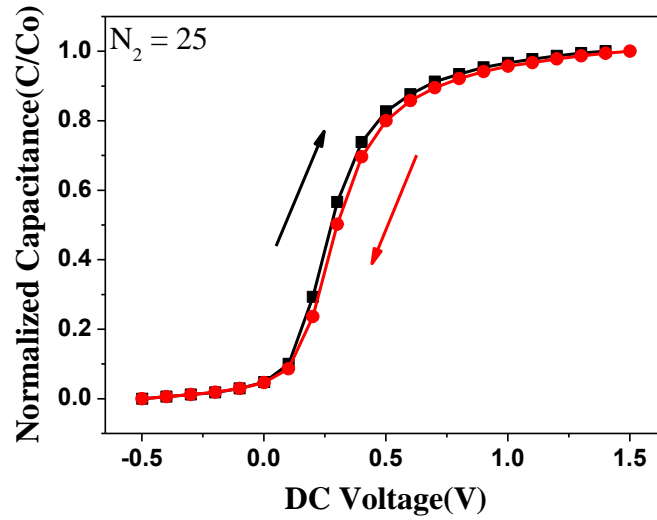
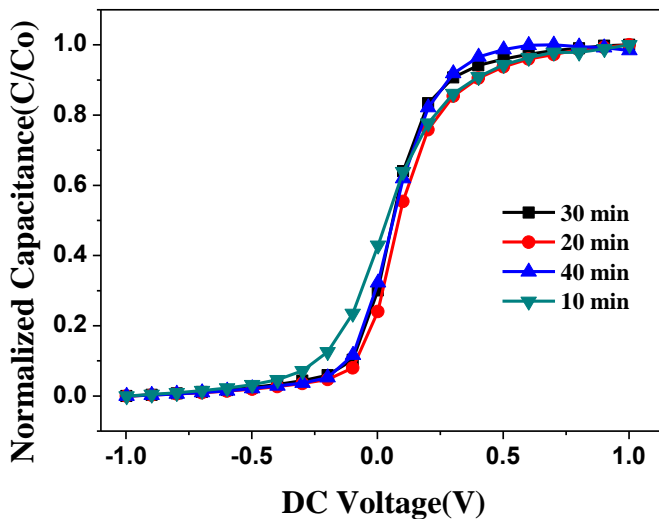


Fig 3-10: Effect of sweep direction for annealed samples with flow rate

3.2.2 Influence of thickness on Si/TiN interface

Variation of thickness could modify the interface in terms of the fixed charges, defects as a result of extended interaction of plasms with film being deposited. In order understand such effects TiN films were deposited for the different time intervals and evaluated the MIS device parameters. It could be understood from the C-V curves that the as-deposited films did not show the flat band shift with respect to thickness. After hydrogen annealing, positive shift could be observed with the increase of thickness, inferring that the hydrogen generated defects that traps negative charges.

As Deposited



Annealed

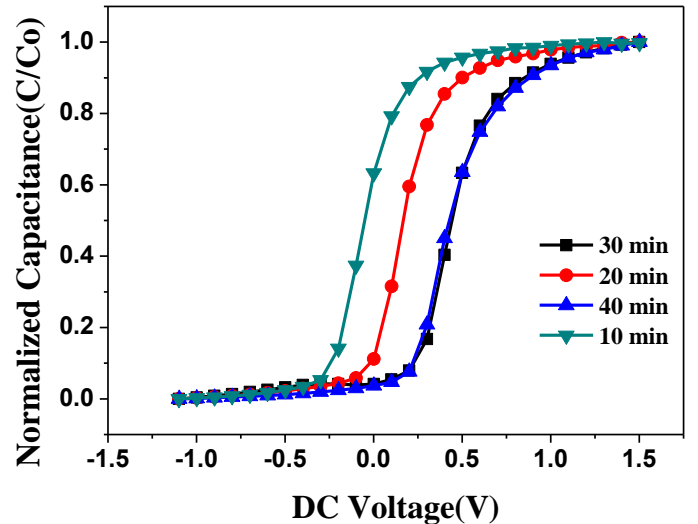


Fig 3-11 :Comparison of C-V as deposited and annealed with variation in time

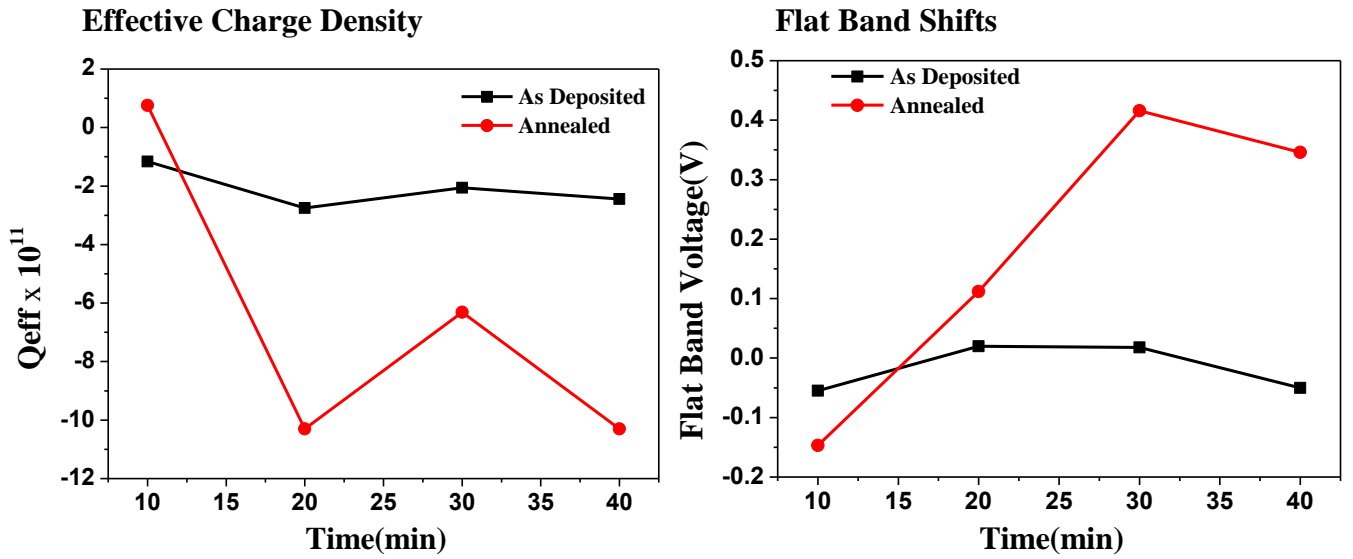


Fig 3-12:Trends in as deposited and annealed for (a) Effective Charge Density (b) Flat band shift with time

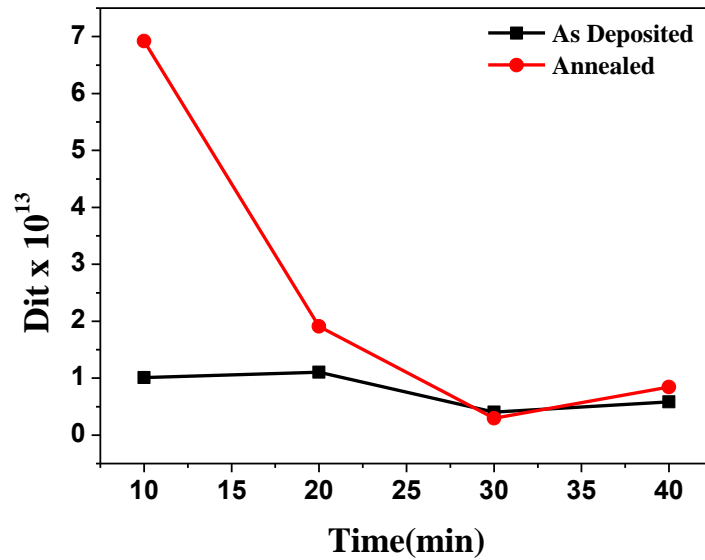


Fig 3-13 : Dit values for different deposition time.

Table3-2 : Q_{eff} , V_{fb} , Dit values for as deposited and annealing for variation in deposition time

| Sl No. | Time (min) | As deposited Q_{eff} ($C.cm^{-2}$) | As Deposited V_{fb} (V) | As Deposited Dit ($cm^{-2}eV^{-1}$) | Annealed at 400°C Q_{eff} ($C.cm^{-2}$) | Annealed at 400°C V_{fb} (V) | Annealed at 400°C Dit ($cm^{-2}eV^{-1}$) |
|--------|-------------|--|---------------------------|---|---|--------------------------------|--|
| 1. | 10 | -1.16×10^{11} | -0.055 | 1.01×10^{13} | 7.56×10^{10} | -0.147 | 6.91×10^{13} |
| 2. | 20 | -2.75×10^{11} | 0.02 | 1.10×10^{13} | -1.03×10^{12} | 0.112 | 1.91×10^{13} |
| 3. | 30 | -2.06×10^{11} | 0.018 | 4.02×10^{12} | -6.31×10^{11} | 0.416 | 2.96×10^{12} |
| 4. | 40 | -2.44×10^{11} | -0.005 | 5.81×10^{12} | -1.03×10^{12} | 0.346 | 8.41×10^{12} |

Fig.3-11 (1Mhz), shows the normalized high frequency(1Mhz) C-V curves of as deposited and annealed samples. The curve behaviour varies with different deposition time which is supported by the change in flat

band voltage of the as deposited samples from fig 3-12(b). all the flat band voltage for all the samples lies in the positive bias range. This confirms the presence of negative fixed charge carriers in the as deposited one. Fixed charges of the order 10^{11} cm^{-3} are obtained for all the samples at irrespective of deposition condition. For Samples with deposition time $< 30 \text{ min}$ poor interface is obtained, characterized by interface trap density of the order of $10^{13} \text{ cm}^{-2}/\text{eV}$. (Fig 3.13) one can conclude that post deposition annealing did not change much interface quality. For time 30 mins D_{it} of the order of $10^{12} \text{ cm}^{-2}\text{eV}^{-1}$. Hence the effect of chemical passivation can be seen more on 30 min time than the others.

3.2.2.1 Influence of annealing

The variation of defects/fixed charges at the interface was analysed by annealing the devices under H_2 ambience. It was observed that the C-V curve shifted positively after hydrogen annealing, indicating that H_2 annealing induced negative fixed charges in the dielectric film. However, for the films deposited at $\text{N}_2=10 \text{ SCCM}$, the shift is nominal, representing the lower interface defect density as seen from the variation of defect density with respect to N_2 flow. As a result, hydrogen might not have form allotropic forms of H^{3+} .

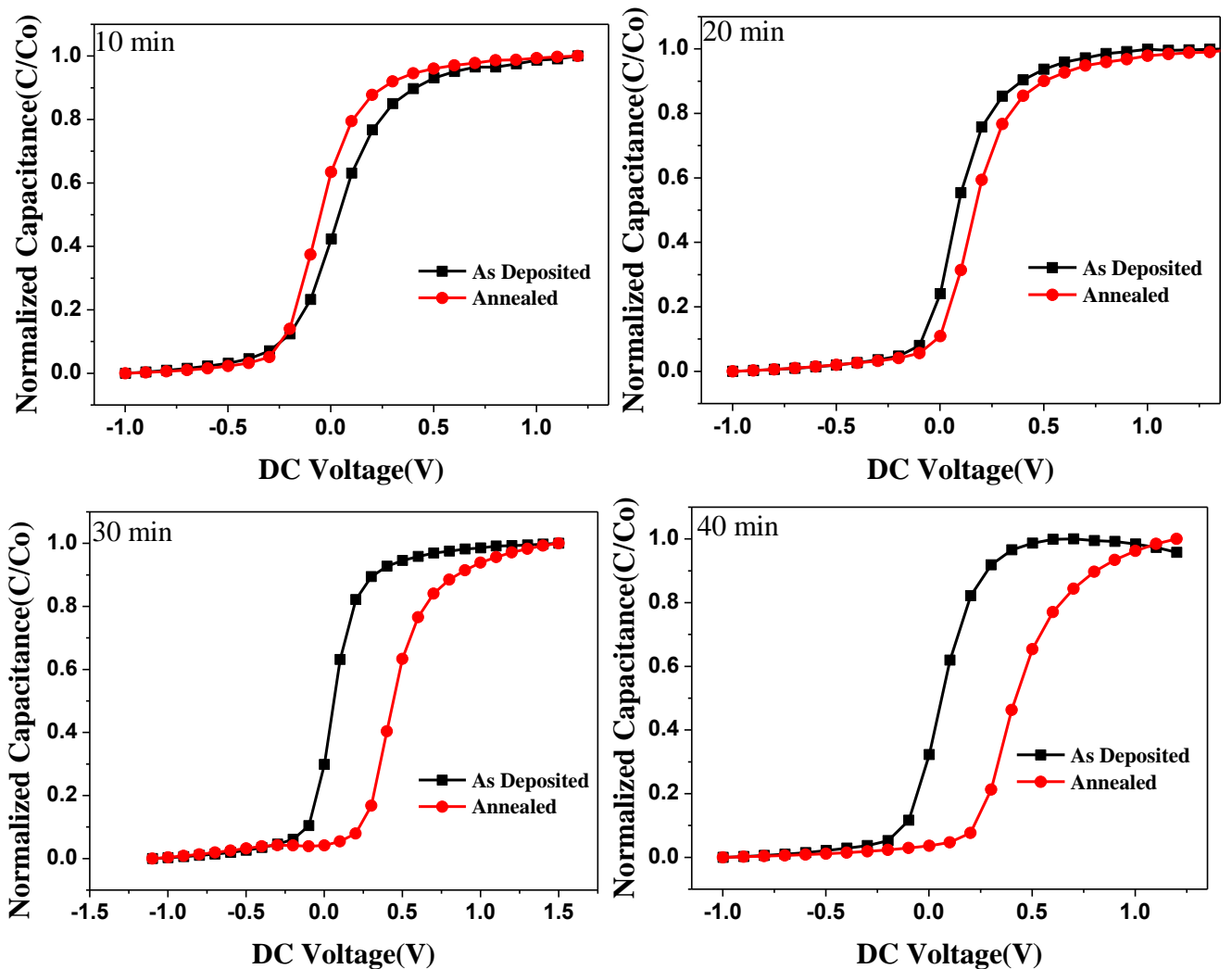


Fig 3-14: C-V for as deposited and annealed at 1MHz with deposition time variation

3.2.2.2 Nature of traps

Frequency dispersion the C-V spectrum of the devices for different thicknesses shows the nature of defects changes with respect to the film thickness. It can be observed from the figures that the sample deposited for 30 min showed lower defect density among the films deposited.

As Deposited

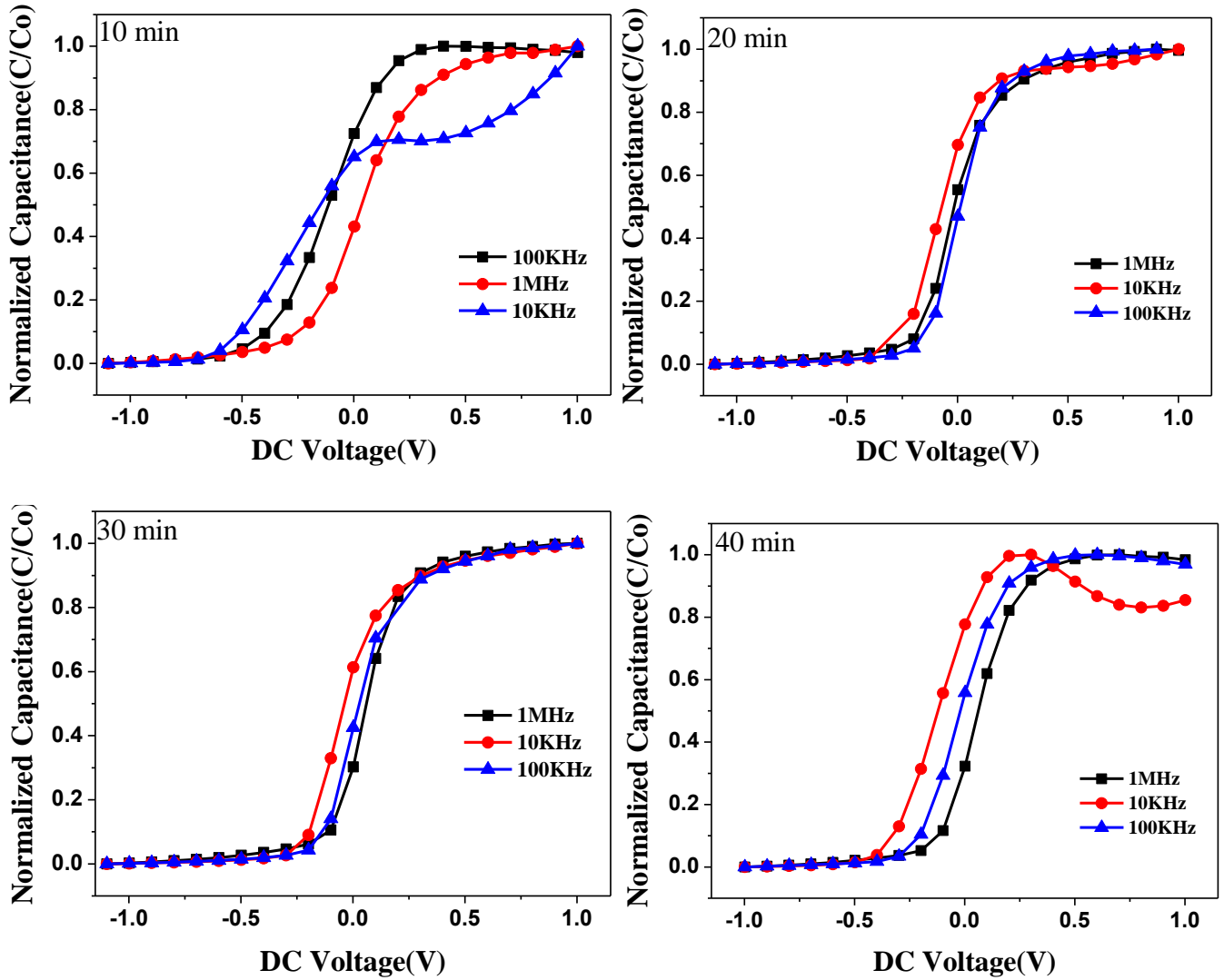
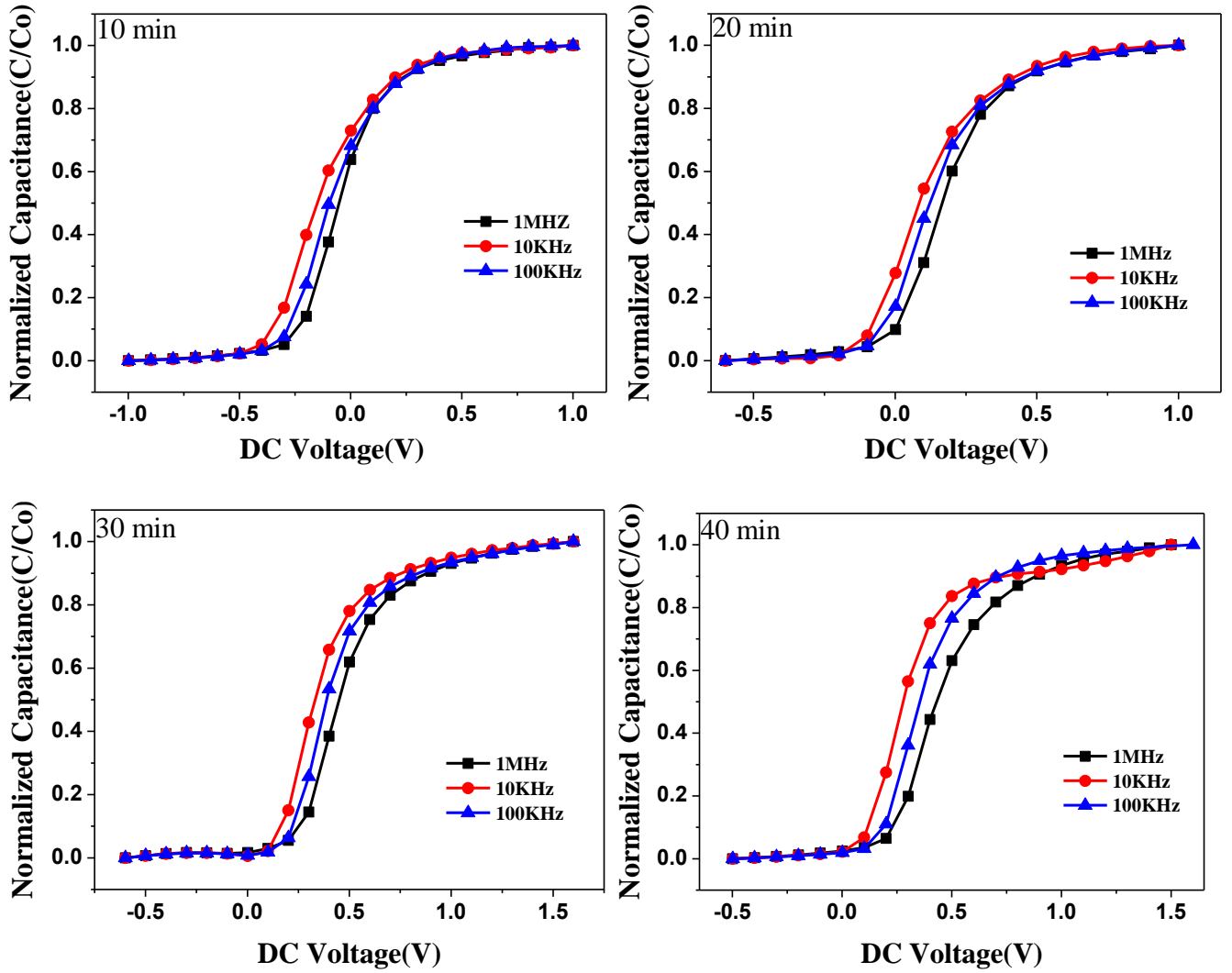


Fig 3-15 C-V curve with different frequency variation for as deposited samples with deposition time

Annealed

As seen from the following figures, the films showed frequency dispersion in the flat-band voltage, irrespective of the film thickness, representing the presence of defects at the interface after annealing in hydrogen.

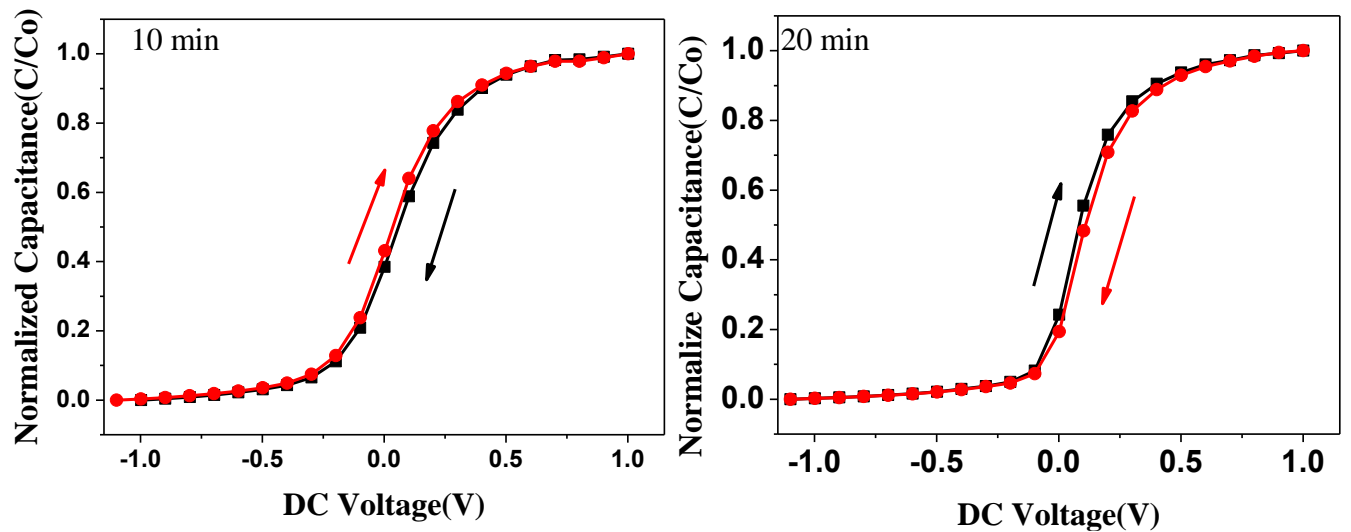
Fig 3-16: C-V curve with different frequency for annealed samples with deposition time



3.2.2.3 Effects of Trap at the interface.

As observed from the following figures, the interface defects are fast traps and its nature did not change with respect to thickness as well as hydrogen annealing.

As Deposited



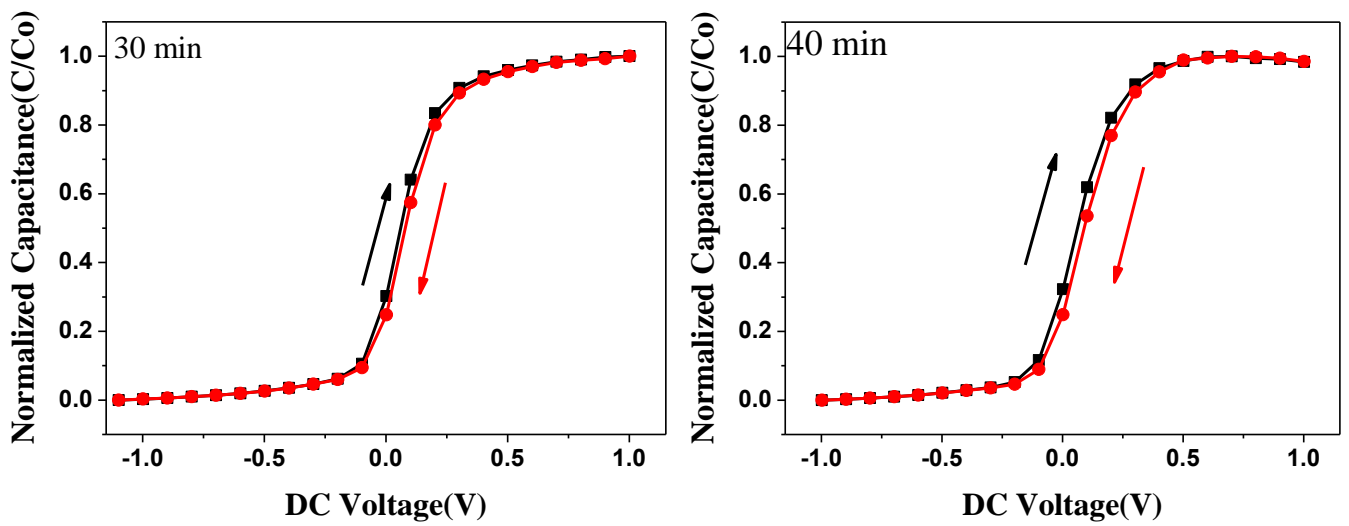


Fig :3-17 :Effect of sweep direction for as deposited with change in deposition time

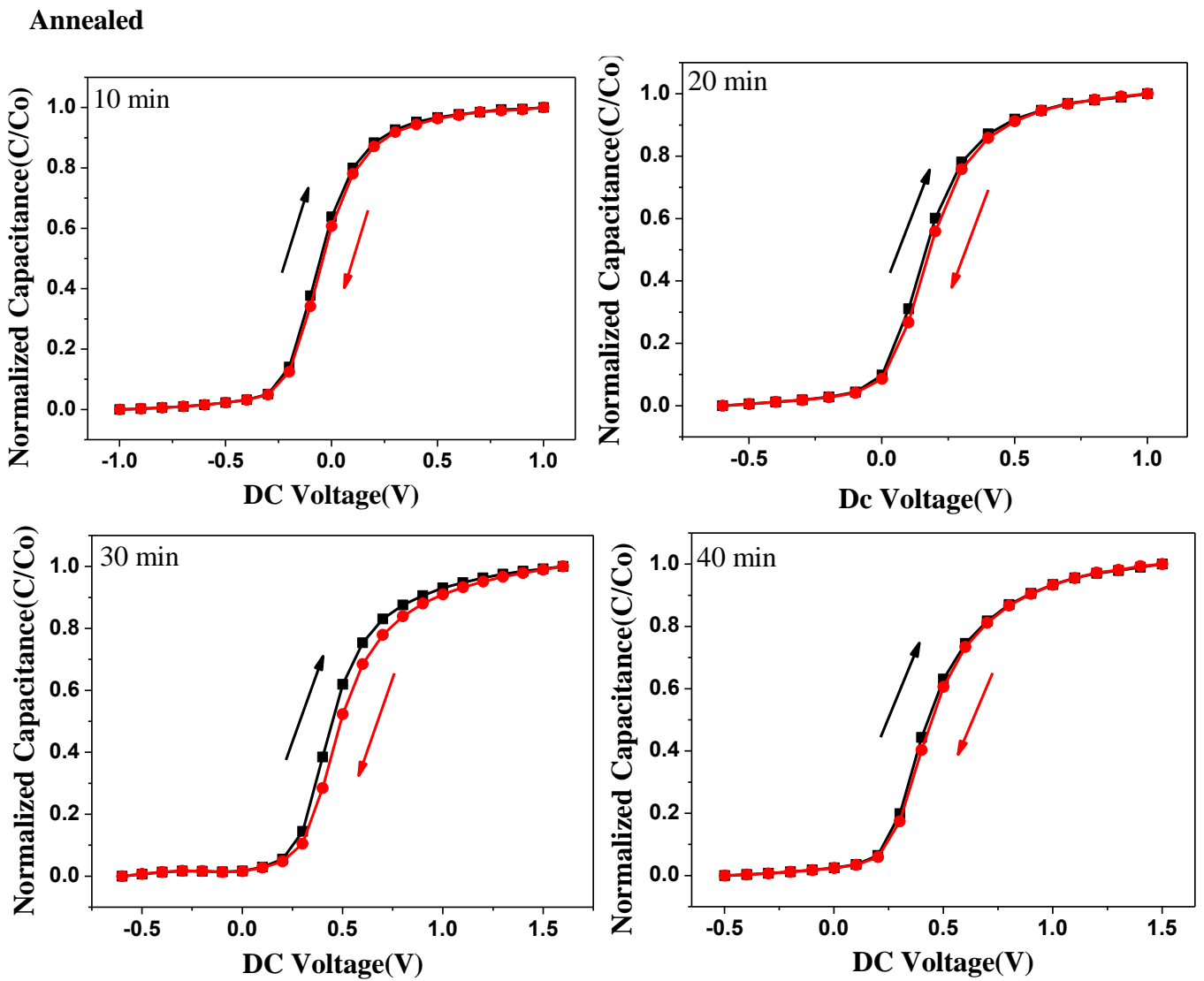


Fig 3-18 : Effect of sweep direction for annealed with change in deposition time

3.2.3 Leakage Current Characteristics

The current-voltage characteristics are shown in figure for different N₂ flows and thicknesses. The devices have shown minimum leakage current at the optimum flow rates of 10-15 SCCM, and at the thicknesses of the films deposited for > 30 min.

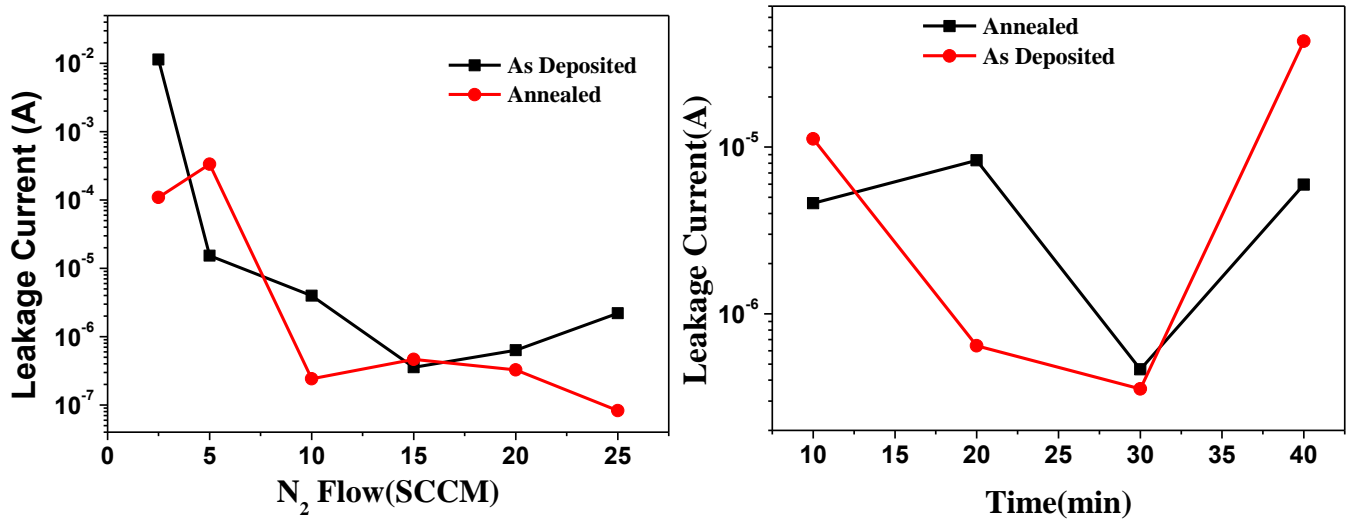


Fig 3-19 : Leakage Current variation with (a) nitrogen flow rate and (b) deposition time for as deposited and annealed

Table 3-3 : Values for leakage current for different Nitrogen Flow

| Sl.No | N ₂ Flow (SCCM) | Leakage Current (A) As Deposited | Leakage Current(A) Annealed |
|-------|----------------------------|----------------------------------|-----------------------------|
| 1. | 2.5 | 1.133×10^{-2} | 1.093×10^{-4} |
| 2. | 5 | 1.533×10^{-5} | 3.332×10^{-4} |
| 3. | 10 | 3.965×10^{-6} | 2.425×10^{-7} |
| 4. | 15 | 3.545×10^{-7} | 4.646×10^{-7} |
| 5. | 20 | 6.303×10^{-7} | 3.262×10^{-7} |
| 6. | 25 | 2.195×10^{-6} | 8.275×10^{-8} |

Table 3-4 : Values for Leakage Current for different deposition time

| Sl.No | Time (min) | Leakage Current (A) As Deposited | Leakage Current(A) Annealed |
|-------|------------|----------------------------------|-----------------------------|
| 1. | 10 | 1.119×10^{-5} | 4.601×10^{-6} |
| 2. | 20 | 6.44×10^{-7} | 8.337×10^{-6} |
| 3. | 30 | 3.545×10^{-7} | 4.646×10^{-7} |
| 4. | 40 | 4.31×10^{-5} | 5.955×10^{-6} |

CHAPTER-4

Passivation Effect of Sputtered Deposited TiN Layer

4.1 Introduction

TiN is promising coating material with technically interesting characteristics such as high thermal and electric conductivity, high corrosion and reflectivity, high wear resistance and melting point, and ultrahigh hardness etc. TiN layers are used in different applications, e.g., as wear and corrosion resistant layers, as biocompatible layers for implants, as diffusion barriers for electronic devices, as optical layers etc.

Based on thermodynamic predictions electrochemically induced oxidation of TiN has been well studied by several groups [35-42]. TiN immersed in aqueous solution shows stability. Meyer et al. [40] observed high stability of TiN up to 1.3V/SHE during electrochemical oxidation. The cause of this high stability was attributed by a nitric anionic surface that protects the underlying Ti atoms. On the other hand another report shows that stability of TiN in aqueous solutions up to 1.25V/SHE and above this it oxidized to nohydrous TiO_2 [41]. In a further study by Knotek et al. [42] it was found that electrochemical stability of TiN is up to 1.3V/SHE and above this TiN oxidized to TiO_2 .

In this chapter other than this protective and stable property of TiN layer the passivation of Si surface by the TiN layer has been investigated. On the best of our knowledge this type of study is rare in literature. It has been found that the short circuit current density (J_{SC}) of the solar cells has been increased by 2.5 times however the V_{oc} shows a slight increment.

4.2 Experiment

4.2.1 Preparation of Silicon Solar Cell

Solar cell is prepared on 300 μm thick p-type (100) single side polished crystalline p-Si substrates with resistivity of 5-10 ohm-cm. The Si substrates were cleaned with acetone (10 min) and ethanol (10 min) by sonication and then rinsed with deionized water 2–3 times and boiled in a 4:1 mixture of H_2SO_4 (96%) and H_2O_2 (30%) for 15 min and rinse by (deionised) D. I. Water thoroughly. After dipping in 2% HF for 2 minute immediately the P507 (phosphorous dopant solution) has been spin coated on the planar substrate. After the spin-coating the substrates were heated at 90°C for 10 min on the hot plate and at 200°C in oven for 15 min. After that we used the diffusion furnace to diffuse Phosphorus on the front surface at 990°C for a chosen time period. Diffusion of dopant creates PSG layer. Now to remove PSG these Si substrates were dipped in 2% HF solution for 5 min and thoroughly washed by deionized water.

For fabrication of Al electrode on the back surface electron beam evaporator at a base pressure $\sim 3 \times 10^{-6}$ mbar was used. Thickness of the electrode was kept around 1 μm . After deposition of back contact BSF

formation was achieved. Ag electrode in finger grid pattern was deposited by electron beam evaporator at a base pressure $\sim 3 \times 10^{-6}$ mbar. Contact sintering was done after that to achieve ohmic contact. The effective area of the solar cells was kept at 1 cm^2 .

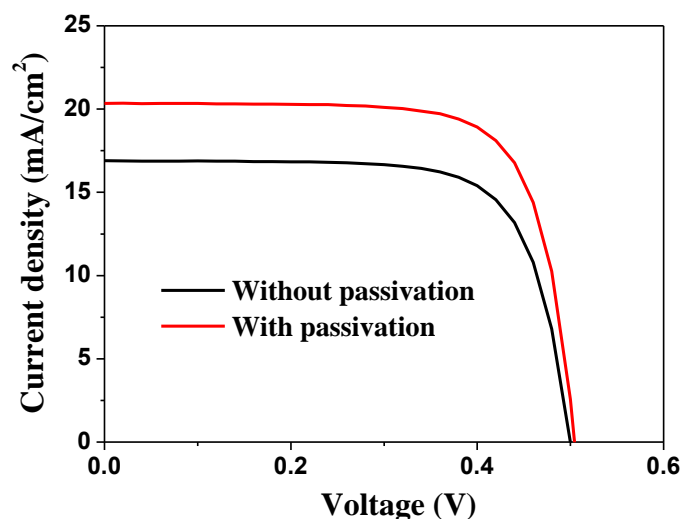
Solar Cells were coated with the optimized condition of Titanium thin film. One sample is annealed at 400°C .. To compare the effect of passivation between the as deposited solar cells and the annealed solar cell, I-V , EQE measured is performed before deposition of layer and then after deposition .

4.2.2 Device Characterization

J-V and EQE characterizations were performed through M/s Bunkoukeiki system.

4.3 Results and Discussion

Sample S2 : As deposited



Sample S1 : Annealed

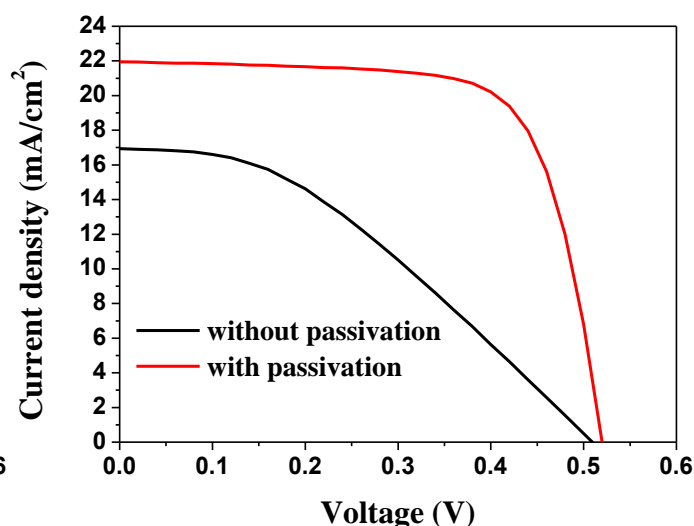


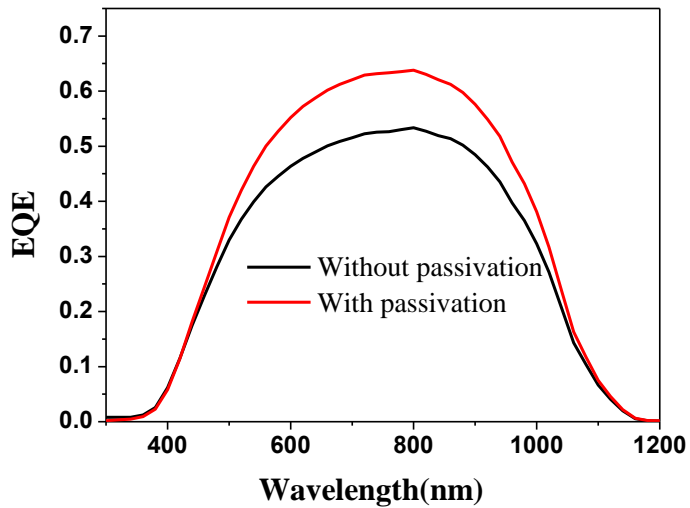
Fig 4-1 : Current density Vs. voltage characteristics of solar cells (a) without passivation and with passivation (as deposited) (b) without passivation and with passivation (annealed) under AM1.5G solar

Fig:4-1 shows current density vs. voltage characteristics of the as deposited and annealed solar cells with passivation layer and without passivation layer. Table shows the solar cell parameters of this cells, form table 1 and figure it is clear that the passivation effect of TiN increases with annealing. This enhancement is more for Jsc however Voc shows little change. For annealed sample Jsc increases from 16.94 to 21.95 mA/cm^2 . But in case of as deposited sample Jsc has been found to increase from 16.91 to 20.34 mA/cm^2

Fig: shows EQE of the same samples. Every samples shows a broad EQE , here in this case also annealed samples shows higher EQE than the as deposited one and both shows higher values than the unpassivated samples. For short wavelengths the annealed samples shows higher EQE values than the as deposited one,

it could be attributed to the fact that the dangling bond related surface defects are strongly passivated by the annealing effect . This passivation effect enhances the efficiency of the solar cell by 2.5 times.

Sample S2 : As deposited



Sample S1 : Annealed

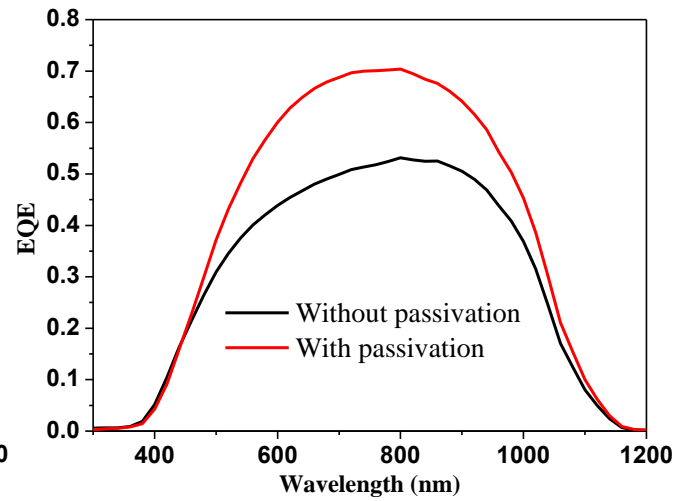


Fig 4-2 : EQE of solar cells (a) without passivation and with passivation (as deposited) (b) without passivation and with passivation (annealed) under AM1.5G solar illumination

Table 4-1: Solar Cell Parameters of passivated and without passivated solar cells

| Sample | Passivation | Jsc (mA/cm ²) | Voc (V) | FF | η (%) |
|--------|-------------|------------------------------|------------|-------|------------|
| S1 | No | 16.94 | 0.51 | 0.37 | 3.196 |
| „ | Yes | 21.95 | 0.52 | 0.713 | 8.14 |
| | | | | | |
| S2 | No | 16.91 | 0.5 | 0.73 | 6.17 |
| | Yes | 20.34 | 0.504 | 0.74 | 7.58 |

Conclusion and Future Work.

Conclusion

The TiN layer has been deposited by using DC Magnetron Sputtering with various nitrogen flow rate starting from 2.5(SCCM) to 25(SCCM). It has been found during the optical characterization that the transmission of the film was low for nitrogen flow rate 2.5- 5 (SCCM). However, for the films deposited by using 10 SCCM nitrogen flow rate show much higher transmittance and further increase in flow rate shows slight increment in the transmittance property. Time of deposition is also varied for a particular flow rate(15SCCM) and it has been found that with increase of deposition time, transmittance decreases.

Defects analysis has been carried out on as deposited and annealed TiN films with different nitrogen flow rate and deposition time. It has been found that for as deposited conditions, interface defect density(Dit) is lowest ($4.02 \times 10^{12} \text{ cm}^{-2} \text{ eV}^{-1}$) for flow of 15 SCCM as compared to other flow rates. The values of negative fixed charge density(Qeff) is also found to be least for flow rate of 15 SCCM. For hydrogen annealed samples, Dit values is lower or within the flow rate of 10 -15 SCCM.. Dit value for 15 SCCM is further reduced to $2.96 \times 10^{12} \text{ cm}^{-2} \text{ eV}^{-1}$ by hydrogen annealing. The Dit value for as deposited samples obtained by using 15 SCCM flow rate is the lowest among other annealed samples of different flow rate. This could help in better chemical passivation. This passivation effect is discussed in Chapter 4. So a flow rate of 15 SCCM has been set. With change in deposition time, the values of Dit is found to be lowest for time 30 min for both as deposited and annealed samples. Leakage current value is lower for the flow rate of 10 – 15 SCCM and for deposition time >30 min. This shows better dielectric behaviour

This TiN layer has been deposited on planar silicon solar cells and the passivation effect has been studied for as deposited TiN layer and annealed TiN layer. It has been found that for annealed TiN layers the passivation effect has increased the Jsc value by 2.5 times and has a little effect on Voc. Fill Factor also improves in presence of this passivation layer.

Future Works.

The above work is extended to many different experiments. To study the effect of in-situ annealing (in presence of hydrogen) of TiN films and to characterize the same way by comparing its surface defects parameters by preparing MIS device. After that depositing over solar cell to see the passivation quality from I-V and EQE curves. Also to analyse the effect of cumulative annealing of the same sample and study its influence on the passivation quality of solar cells.

References

1. BP Energy Outlook-2018.
2. Solar Energy Perspectives: Executive Summary" (PDF). International Energy Agency. 2011. Archived from the original (PDF) on 3 December 2011.
3. Energy". *rsc.org*. 2014-04-02.
4. <https://www.pveducation.org/pvcdrom/solar-cell-operation/solar-cell-structure>
5. <https://www.pveducation.org/pvcdrom/design-of-silicon-cells/optical-losses>
6. <https://www.pveducation.org/pvcdrom/design-of-silicon-cells/recombination-losses>
7. SS Sandeep, PhD thesis, "Novel plasma process for surface passivation and light trapping in crystalline solar cell", 2016,
8. Chaoquan Hu, Yuan Tian, Weitao Zheng.' A Review of Corrosion-Protective Transition Metal Nitride Coatings', Vol1. 2015
9. B. Zega, M. Kornmann, J. Amiguet "Hard decorative TiN coatings by ion plating" *Thin Solid Films* 4, 577-82 (1977).
10. Yu Zhong "Transition Metal Carbides and Nitrides in Energy Storage and Conversion", February 2016.
11. Mori, JC, Serra, P, Mart'inez, E, Sardin, G, Esteve, J & Morenza, JL 1999, 'Surface treatment of titanium by Nd:YAG laser irradiation in the presence of nitrogen *Appl. Phys. A* 69 [Suppl.]', pp. S699–S702 .
12. Patrick R LeClair 1998, 'Titanium Nitride Thin Films by the Electron Shower Process by submitted to the Department of Materials Science and Engineering in partial fulfillment of the requirements for the degree of Bachelor of Science in Materials Science and Engineering at the MASSACHUSETTS INSTITUTE OF TECHNOLOGY'.
13. Kavita A, PhD thesis, "Synthesis and Characterization Of Titanium/Titanium Nitride Thin Films Prepared By DC Reactive Magnetron Sputtering With Supported Discharge", Anna University, 2017
14. Ph. Roquiny *, F. Bodart, G. Terwagne, "Colour control of titanium nitride coatings produced by reactive magnetron sputtering at temperature less than 100°C", *Surface and Coatings Technology* 116–119 (1999) 278–283.
15. Mühlbacher M, Thesis "High-resolution characterization of TiN diffusion barrier layers", Linköping University, 2015.
16. S.M Sze, Kwok "Physics of Semiconducting Devices" Wiley Publication, Third Edition.
17. Schroder D.K, "Semiconductor Material and Device Characterization", Wiley-IEEE Press, 2006.

18. Khairnar A.G, PhD thesis "Deposition and characterization of high-k dielectric thin films for MOS capacitor", N.M.U Jalgaon, 2014.
19. Krishna Seshan, Handbook of Thin-Film Deposition Processes and Techniques, 2nd Ed. Noyes Publications, 2002
20. https://ethw.org/Thin_Film_Deposition_Technologies
21. Michael Faraday, Phil. Trans. R. Lond., 147, 145-181, 1857
22. R.F. Bunshah, Handbook of deposition technologies for films and coatings, Noyes Publication (1994) New Jersey
23. R.N. Ghoshtagore, J. Electrochem. Soc., 125 (1978) 110.
24. G.A. Prinz, Science, 250 (1990) 1092.L
25. S. K. Ghandhi, VLSI Fabrication Principles, 2nd Ed. John Wiley & Sons, 2012
26. Stephen A. Campbell, The Science and Engineering of Microelectronic Fabrication, Oxford University Press New York, 1996
27. , B. Chapman, Glow Discharge Processes, John Wiley & Sons, New York, 1980
28. https://www.iitk.ac.in/ibc/Vacuum_Gauges.pdf
29. <https://m.youtube.com/watch?v=TG9vtKK-LLw>
30. Vipin Chawla, Jayaganthan R, Chawla, AK & Ramesh Chandra 2009 'Microstructural characterizations of magnetron sputtered Ti films on glass substrate', Journal Of Materials Processing Technology, vol. 209, no. 7, pp. 3444-3451.
31. web.iitd.ac.in/~sdeep/Electronic.pdf
32. Perkin Elmer Lambda 1050 Instrument manual.
33. Reference 600 Operators Manual
34. <https://www.pveducation.org/pvcdrom/solar-cell-operation/quantum-efficiency>
35. B. Elsener, A. Rota, and H. Böhni, Mater. Sci. Forum, 44/45, 29 (1989).
36. M. Herranen, M. Nordin, and J.-O. Carlsson, J. Vac. Sci. Technol. B, 15, 1865 (1997).
37. A. K. Gorbachev, Prot. Met., 19, 212 (1983).
38. J. C. François, Y. Massiani, P. Gravier, J. Grimblot, and L. Gengembre, Thin Solid Films, 223, 223 (1993).

39. I. Milosev, H.-H. Strehblow, B. Navinsek, and M. Metikos-Hukovic, *Surf. Interface Anal.*, 23, 539 (1995).
40. . B. Siemensmeyer, K. Bade, and J. W. Schultze, *Ber. Bunsenges. Phys. Chem.*, 95, 1461 (1991).
41. N. Heide and J. W. Schultze, *Nucl. Instrum. Methods Phys. Res.*, B80/81, 467 (1993).
42. . O. Knotek, A. Schirley, J. W. Schultze, and B. Siemensmeyer, *Werkst. Korros.*, 43, 511 (1992)